Technical Report No. 16

COMPARISON OF DROUGHT INDICES FOR THE PROVINCE OF GELDERLAND, THE NETHERLANDS

Author names: Jurriaan ten Broek, Adriaan J. Teuling, Anne F. Van Loon

Date: 1 September 2014

DROUGHT-R&SPI (Fostering European Drought Research and Science-Policy Interfacing) is a Collaborative Project funded by the European Commission under the FP7 Cooperation Work Programme 2011, Theme 6: Environment (including Climate Change, ENV.2011.1.3.2-2: Vulnerability and increased drought risk in Europe (Grant agreement no: 282769). The DROUGHT-R&SPI project started 01/10/2011 and will continue for 3 years.

Title:	COMPARISON OF DROUGHT INDICES FOR THE PROVINCE OF GELDERLAND, THE NETHERLANDS
Authors:	Jurriaan ten Broek, Adriaan J. Teuling, Anne F. Van Loon
Organisations:	Wageningen University, Wageningen, the Netherlands
Submission date:	1 September 2014
Function:	This report is an output from Work Package 1; Task 1: Quantitative analysis of historic large-scale droughts in Europe
Deliverable:	This report contributes to DROUGHT-R&SPI deliverable D1.5 Evaluation of the potential and limitations of pan-European analyses across scales

Photo made by Jurriaan ten Broek

Acknowledgement/Preface

The first author has carried out this study as part of the MSc programme Earth and Environment, specialization Hydrology and Quantitative Water Management, Wageningen University, Wageningen, The Netherlands. In addition to the DROUGHT-R&SPI project, the research contributes to the programme of the Wageningen Institute for Environment and Climate Research (WIMEK-SENSE) and it supports the work of the UNESCO-IHP VIII EURO FRIEND Water programme.

We thank the organisations that provided the data for this study, i.e. the Royal Dutch Meteorological Institute KNMI for the meteorological data, TNO for the groundwater data (DINOloket), Rijkswaterstaat and the waterboards Rijn en Ijssel, De Dommel, Brabanste Delta, Regge en Dinkel, Roer en Overmaas, Hunze en Aa´s, and Velt en Vecht for the discharge data and Niko Wanders of Utrecht University for the satellite soil moisture data.

We also thank P.J.J.F. Torfs and H.A.J. Van Lanen for providing technical guidance and theoretical background.

Wageningen, September 2014

Abstract

Even though The Netherlands is generally seen as a wet country, droughts can cause severe problems. Significant drought conditions are observed in the index based on precipitation and potential evaporation by the Royal Dutch Meteorological Institute (KNMI). In this study the spatial and temporal variability of meteorological and hydrological drought indices has been investigated. We were interested to see if the KNMI can capture the propagation of meteorological drought into hydrological drought. The Standardized Precipitation Index (SPI), the Standardized Precipitation Evapotranspiration Index (SPEI), the Standardized Runoff index (SRI), the Standardized Water Level Index (SWI, groundwater) and the Soil Moisture Anomalies (SMA) were used to quantify drought in the province of Gelderland, The Netherlands, at multiple time scales within the period 1988-2013. The results indicate that drought indices based on different variables show the same major drought events. Drought indices based on precipitation and potential evaporation are more variable in time while drought indices based on discharge and groundwater have a smoothed signal. Spatial distribution of meteorological drought is uniform over Gelderland, whereas large spatial variation exists in hydrological drought (groundwater). Areas with deep groundwater tables experience still wet conditions during selected drought events, caused by the slow response to changes in precipitation. Runoff measurements are less useful for spatial analysis of drought because of limited spatial coverage and short length of the available data. Due to differences in temporal and spatial variation, meteorological drought indices (like the index used by KNMI) cannot simply be used to represent hydrological drought conditions.

Key words: Drought, Drought propagation, SPI, SPEI, SRI,SWI, Spatial variation

Table of Contents

List of Tables

List of Figures

1 Introduction

According to the fifth assessment report of the Intergovernmental Panel on Climate Change (IPCC) climate change is likely to increase the frequency of meteorological droughts (less rainfall) and agricultural droughts (less soil moisture) in presently dry regions by the end of this century. This is likely to increase the frequency of short hydrological droughts (less surface water and groundwater) in these regions. There is no evidence that surface water and groundwater drought frequency has changed over the last few decades, although impacts of drought have increased mostly due to increased water demand (IPCC, 2014). This conclusion is based on global scale modelling by a large number of scientists. During the last century a number of intense drought events affected societies around the world. Droughts have a significant social, economic and environmental impact with direct and indirect effects such as power cuts, transport problems, loss of agriculture production and forest fires. Examples of these impacts of droughts are described in Tallaksen and Van Lanen (2004). Monitoring of time series of discharge, groundwater and soil moisture is very useful because with this information it is possible to monitor and study drought, recognise spatial patterns and analyse trends in the observed data. An important characteristic is for example the lowest groundwater level as result of the seasonality. This knowledge could be applied for agriculture and nature conservation. Hydrological drought usually develops from a water deficit at the surface that is larger than normal. In The Netherlands the Royal Netherlands Meteorological Institute (KNMI) measures the cumulative water deficit based on precipitation and potential evaporation from the 1st of April until the end of September. Low precipitation during winter, the wet season in The Netherlands, may lead to the development of a drought in spring and summer because the groundwater has received no recharge. So already before the 1st of April, severe drought conditions can develop and local groundwater and soil moisture conditions can play a large role in determining the actual water deficit. This thesis is scientifically relevant because in The Netherlands, no monitoring index of drought exists which is based on groundwater, soil moisture and/or discharge. Early droughts in the year (before the 1st of April) should be quantified.

1.1 Objectives

The objective of this study is to quantify drought in The Netherlands based on meteorological observations (precipitation and potential evaporation) and hydrological observations (groundwater, soil moisture and discharge). To see the areas which are vulnerable for periods of drought, special attention will be given to regional differences within the province Gelderland.

The main research questions are:

1. What is the difference between the KNMI drought index and drought indices based on continuous

observations of precipitation, potential evaporation, soil moisture, discharge and groundwater levels?

2. To what extent can a new drought index for The Netherlands be developed based on currently available observations of actual deficiencies in precipitation, potential evaporation, soil moisture, discharge and groundwater levels?

To answer the main research questions the following sub questions are defined:

1a What explains the difference between the historical drought maps of the KNMI compared to the drought indices based on precipitation, potential evaporation, soil moisture, discharge and groundwater levels?

1b How do gaps in data influence the quantification of droughts?

2a How can soil moisture data be used in a drought monitoring system for The Netherlands? Which soil moisture data source is useful?

2b How can groundwater data be used in a drought monitoring system for The Netherlands? How many groundwater data are needed?

2c How can discharge data be used in a drought monitoring system for The Netherlands? Is discharge a useful variable for drought monitoring in The Netherlands?

2d Can a combined drought index based on soil moisture, groundwater and discharge be found that indicates the drought situation in The Netherlands correctly? How does it differ from the KNMI index?

1.2 Outline

In Chapter 2 the theory behind drought is described and definition, origin and propagation, indices and Dutch drought events are discussed. In addition an overview is given of the study region. Chapter 3 describes the input data and the drought indices methods used for the analysis. Furthermore the statistical and interpolation methods are shortly summarised. Chapter 4 shows the results of the several drought indices in Gelderland in comparison with the drought index of the KNMI. The report concludes with a discussion (Chapter 5), conclusion and recommendations (Chapter 6).

2 Background

In Chapter 2 the drought definition, propagation, indices and the Dutch drought events are described. Chapter 2 ends with a description of the study site, with two sections about climatology and hydrology.

2.1 Drought

2.1.1 Definition

Drought is defined as below-average availability of water in the environment. Each drought can be characterised by an onset, duration, severity and intensity. Precipitation, evaporation, snow, humidity, wind and temperature can have important effects on drought conditions. In the next sections of this chapter these climatic factors will be more elaborated. Droughts occur in different climates and are linked to climate variability. The spatial and temporal characteristics vary significantly around the world and vary in every climate (Tallaksen and Van Lanen, 2004).

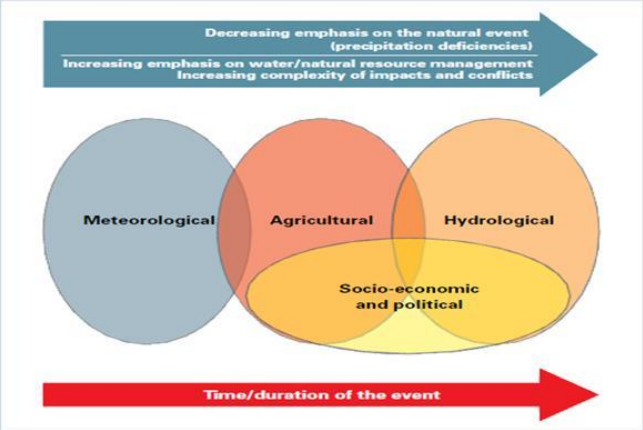

Figure 2.1: Interrelationships between meteorological, agricultural, hydrological and socio-economic drought (Wilhite, 2006).

Four types of drought can typically be distinguished (Figure 2.1):

1. Meteorological drought is a lack of precipitation.
2. Agricultural drought is caused by a lack of precipitation often in combination with high evaporation rates. Agricultural drought is also called soil moisture drought. Infiltration rate and soil characteristics determine the severity.
3. Hydrological drought is related to below-average availability of surface and subsurface water supplies. Recovery is slow because the replenishment by recharge will take a long time (Wilhite, 2006).

4. Socio-economic drought is directly related to the agricultural and hydrological drought. According to Wilhite (2006): “Socio-economic drought reflects the relationship between the supply and demand for some commodity or economic good. Large populations and extensive industrial development will be the most vulnerable”.

2.1.2 Origin and propagation

Most droughts occur when expected precipitation fails and evaporation rates are higher than normal, most times related to sunny and warm conditions (Teuling et al., 2013). High pressure weather systems can be responsible for long term drought events as result of large-scale anomalies in the global circulation pattern of the atmosphere. Winter drought can develop when winter precipitation is stored as snow and does not lead to replenishment of soil moisture, streams and groundwater. Climate factors such as high wind and low relative humidity can contribute to amplify the intensity of a drought (Sönmez et al., 2005). A drought typology was developed by Van Loon and Van Lanen (2012). The occurrence of drought types is determined by climate and catchment characteristics. Precipitation can be considered as the carrier of the drought signal (Figure 2.2). Streamflow (runoff) and groundwater levels can be considered as the last two indicators of the occurrence of a drought (Changnon, 1987). A time lag exists between deficiencies in precipitation and the point where precipitation deficiencies become evident in streamflow and groundwater (Wilhite, 2006).

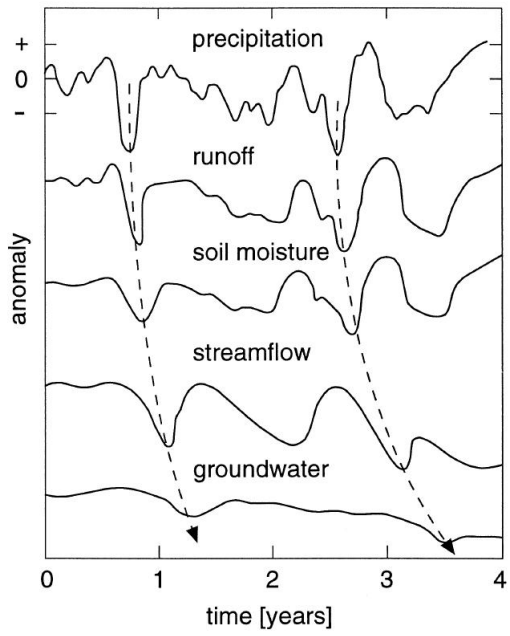

Figure 2.2: Drought propagation in different hydrological variables (Changnon, 1987).

2.1.3 Indices

Drought indices are widely used to quantify drought. In drought analysis most used time scales are year and month. A selection of some commonly used meteorological, agricultural and hydrological drought indices is mentioned. Meteorological indices are the rainfall anomaly index (RAI; Van Rooy, 1965) and rainfall deciles (Gibbs and Maher, 1967). Palmer (1965) developed the Palmer drought severity index (PDSI) which is widely applied in the United States (Hayes et al., 1999). The PDSI has limitations which are well described in Alley (1984) and Hayes et al. (1999). Other examples of agricultural drought indices are the crop moisture index (CMI; Palmer, 1968), the soil moisture deficit index (SMDI) and evapotranspiration deficit index (EDI; Narasimhan and Srinivasan, 2005). Hunt et al. (2009) developed the soil moisture index based on actual water content, measured field capacity and wilting point. Hydrological drought indices are the surface water supply index (SWSI) (Shafer and Dezman, 1982) which deals with the limitations of the PDSI and the groundwater resource index (GRI; Mendicino et al., 2008). Furthermore several studies have focused on how droughts propagate through hydrological systems (Peters et al., 2003, 2006; McEvoy et al., 2012). For a complete overview and comparison of drought indices readers are referred to Heim (2002), Keyantash and Dracup (2002) and Morid et al. (2006).

Standardised indices

Next to the already mentioned drought indices some standardised drought indices exist. They include the standardised precipitation index (SPI; McKee et al., 1993), standardised evapotranspiration index (SPEI; Vicente-Serrano et al., 2009), standardised runoff index (SRI; Shukla and Wood, 2008), the soil moisture anomalies (SMA; Orlowsky and Seneviratne, 2013), standardised water level index (SWI; Bhuiyan, 2004; Bhuiyan et al., 2006) and standardised groundwater index (SGI; Bloomfield and Marchant, 2013). The SPI is only based on precipitation. The SPEI is based on precipitation minus potential evaporation; it has the advantage when selecting the right calculation method to include the effects of temperature variability on drought propagation compared to the SPI. The SRI is based on the assessment of the runoff of a given basin. The SMA takes soil moisture into account. The SWI and SGI (the terms SWI and SGI are used interchangeably in this report) has been developed to monitor anomalies in groundwater levels. Direct comparability is possible between these indices, which makes it a useful and easy way to compare drought events. Because of the normalization, wet and dry climates can be represented in the same way. The advantages of standardised drought indices are the simplicity and the variability in time scales. Disadvantages are the need for long time series of observed data and the need to fit a probability density function (Mishra and Singh, 2010). For multi-year droughts, Guttman (1999) recommends 50 years of data, however, other studies such as McKee et al. (1993) used shorter period of only 30 years. For further information about strengths and weaknesses of all mentioned indices readers are referred to Mishra and Singh (2010) and Wanders et al. (2010).

Low flow indices

Several low flow indices exist, for instance the base flow index (BFI; Institute of Hydrology, 1980), mean annual minimum flow (MAM; Hindley, 1973 and Pirt et al., 1983), percentiles from the flow duration curve (Q70-Q95; Searcy, 1959) and the threshold level (Yevjevich, 1967). The BFI gives the ratio of base flow to the total flow, so a BFI close to 1 indicates high groundwater contribution to streamflow, whereas for ephemeral streams BFI is close to zero (Smakhtin, 2001). A flow duration curve (FDC) is a relationship between any discharge value and the percentage of time that this discharge is equalled or exceeded. MAM is frequently applied as low flow index and the common used time averages are 1--, 7-- and 30--days (Smakhtin, 2001). Yevjevich (1967) already used a kind of threshold level, but with the focus on statistics of analysing time series. Each drought event can be characterised by its deficit volume and duration. The threshold level approach is often used as an index for drought events (Hisdal et al., 2000; Van Loon and Van Lanen, 2012).

KNMI index

The Dutch drought indicator is provided routinely by the KNMI. The interpolated drought map shows the cumulative water deficit based on precipitation minus potential evaporation starting on the 1st of April (Figure 2.3). In the graph the red line indicates the record year 1976, the green line represents the five per cent driest years, the blue line the median, the black solid line the actual precipitation deficit. A decreasing line corresponds to a higher amount of precipitation compared to the potential evaporation and an increasing line shows less precipitation than potential evaporation. When the precipitation deficit is below zero the result of the calculation is stopped. The calculation is continued when there is again a precipitation deficit. In this report the Dutch drought indicator is called “KNMI index”.

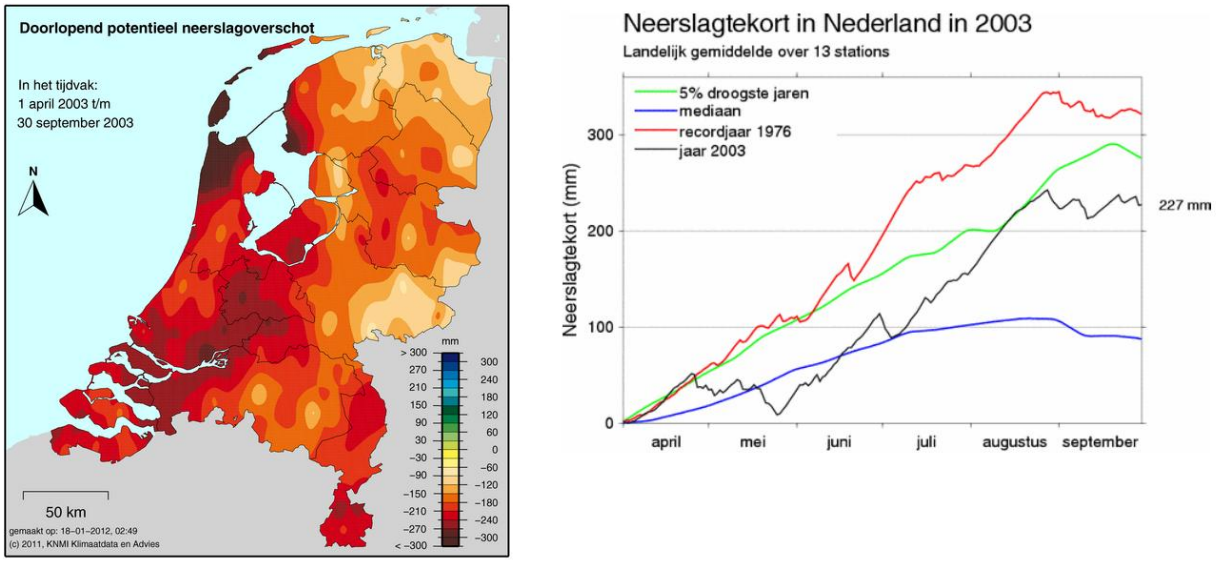

Figure 2.3: The interpolated drought map and a graph which shows the precipitation deficit in time (KNMI, 2014).

Table 2.1: Overview of historic drought events in The Netherlands from 1950 to 2011 (KNMI, 2014)

Period	Drought characteristics
1959	Especially dry during the growing season
1976	Record drought year, especially during the growing season. Precipitation amount was 536 mm (833 mm is the long-term average of 1981-2010)
1995	Especially during the months August and October. No drought during growing season, limited consequences
1996	Especially during the months January till March. No drought during the growing season, limited consequences
Spring 1997	Especially during the months January and March. Limited consequences
2003	A significant dry year, belongs to the 5% of driest years
Summer 2006	Especially during the growing season namely the months June and July
Spring 2007	Drought occurred mostly during the months March, April and May
Spring 2011	Drought occurred during the months April and May

2.2 Study site

The focus in this study is on the province of Gelderland which is situated in the eastern part of The Netherlands. This province has a large variability in soils, landscape features, land-use features and the thickness of the unsaturated zone. From deep groundwater levels to seepage areas.

2.2.1 Geology and climatology

Several ice pushed ridges are present in the landscape, namely the *Veluwe*, *Montferland* and *Berg en Dal* (Figure 2.4). During the ice-age, the *Saalian Stage*, glaciers from Scandinavia pushed unstratified sediment into several ridges. These ridges are high enough to cause a small orographic effect on the precipitation distribution. On average higher precipitation amounts on the *Veluwe* compared to the *Betuwe* (Figure 2.5).

The distribution of potential evaporation shows the opposite compared to the precipitation map: more potential evaporation on average in the *Betuwe* compared to the *Veluwe* area (Figure 2.6). It is important to mention that the absolute differences in potential evaporation are much smaller than the regional differences in the precipitation.

2.2.2 Hydrology

In the higher situated parts of Gelderland, the water is naturally discharged and water fluctuations are caused by seasonal fluctuations of precipitation and evaporation. Drought propagation is relatively natural in these areas. In contrast, in parts of the *Betuwe* and the adjacent western provinces the water flow is

influenced by human activity. When the water discharge is not possible in a natural way, pumping stations help to drain the area. The water is pumped to a so called “boezem”, which is a part of the surface water and has no fixed level. The depth of groundwater table differs between the higher and lower areas (Figure 2.7). The groundwater levels in the *Veluwe*, *Montferland* and *Berg en Dal* are 20 up to 35 meters below surface level, whereas in many other parts the groundwater levels are very close to the surface.

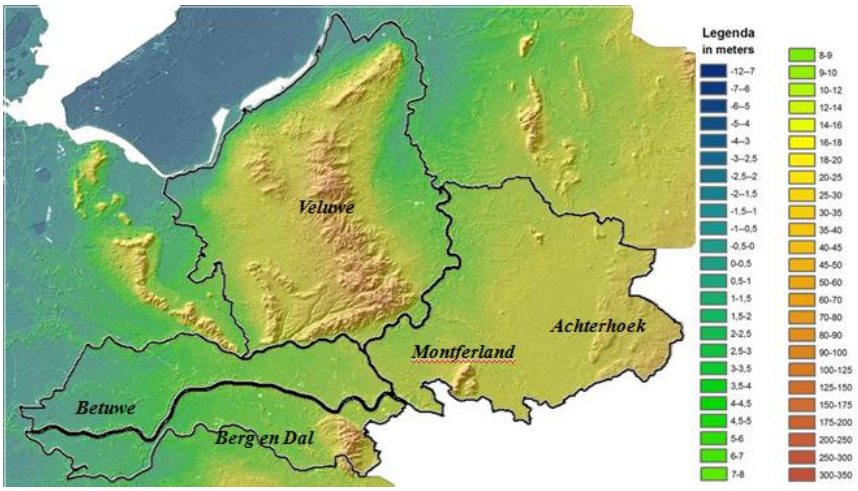

Figure 2.4: Height map of the province of Gelderland (AHN, 2014).

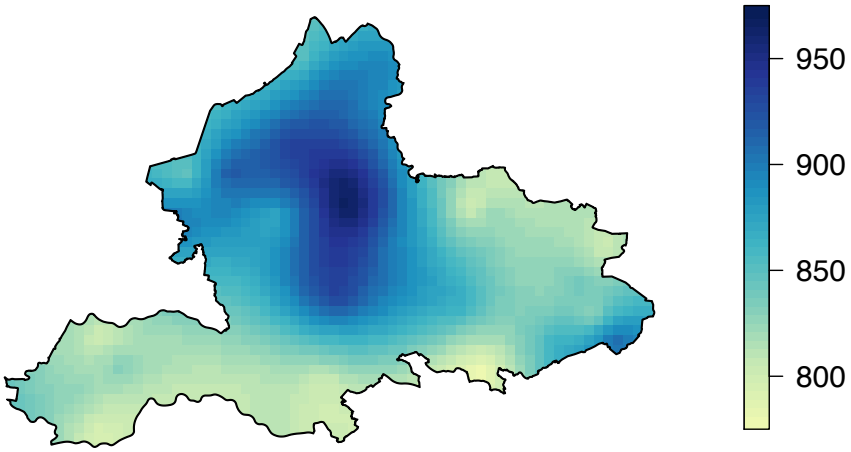

Figure 2.5: Long-term average (1988-2013) of precipitation in the province of Gelderland (KNMI, 2014). The unit is mm / year.

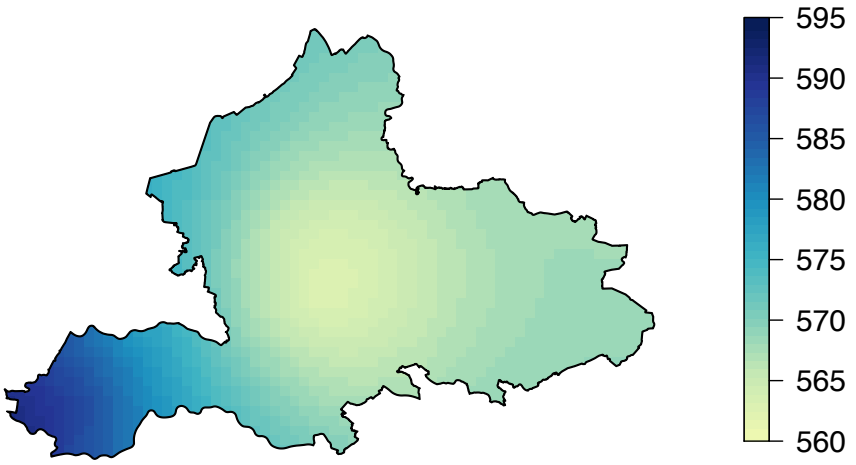

Figure 2.6: Long-term average (1988-2013) of potential evaporation in the province of Gelderland (KNMI, 2014). The unit is mm / year.

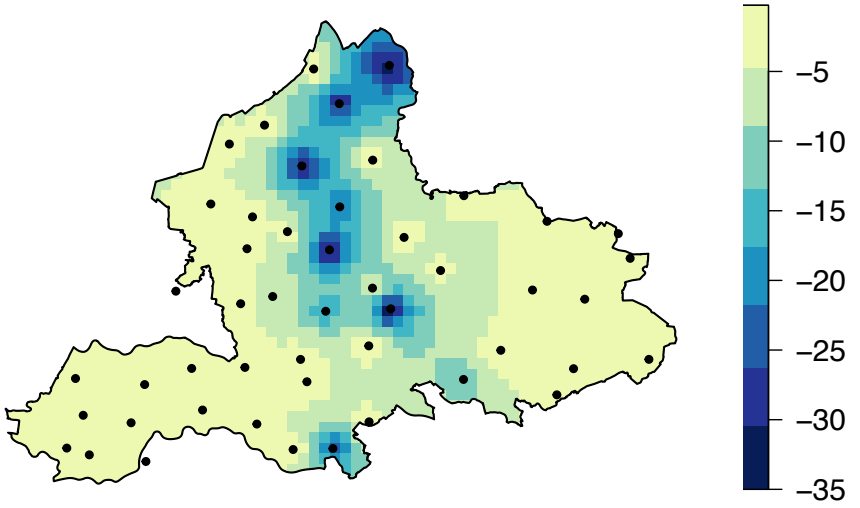

Figure 2.7: Long-term average depth (1988-2013) of groundwater in the province of Gelderland. The black dots indicates the locations of the piezometers (Dinoloket, 2014). The unit is m below surface level.

3 Data and methods

In this chapter, an overview is given of the data which are used in the meteorological and hydrological drought analysis. Furthermore, the different indices to analyse the selected variables namely precipitation, evaporation, soil moisture, runoff and groundwater, are described. The chapter ends with a summary of statistical analyses and spatial interpolation techniques.

3.1 Input data

3.1.1 Precipitation data

Precipitation was used as input variable to calculate meteorological drought. KNMI measures the amount of precipitation with rain gauges on 350 precipitation stations. Two independent rain gauge networks exist: an automatic network of approximately 35 gauges and a manual network of approximately 315 gauges (Appendix A). The 24-h precipitation height from the manual rain gauges is measured at 08.00 UTC. From 1901 till present maps and data are available on `www.knmi.nl`. A total of 51 precipitation stations from the manual network, well spread over the province, were selected from the KNMI (Figure 3.1).

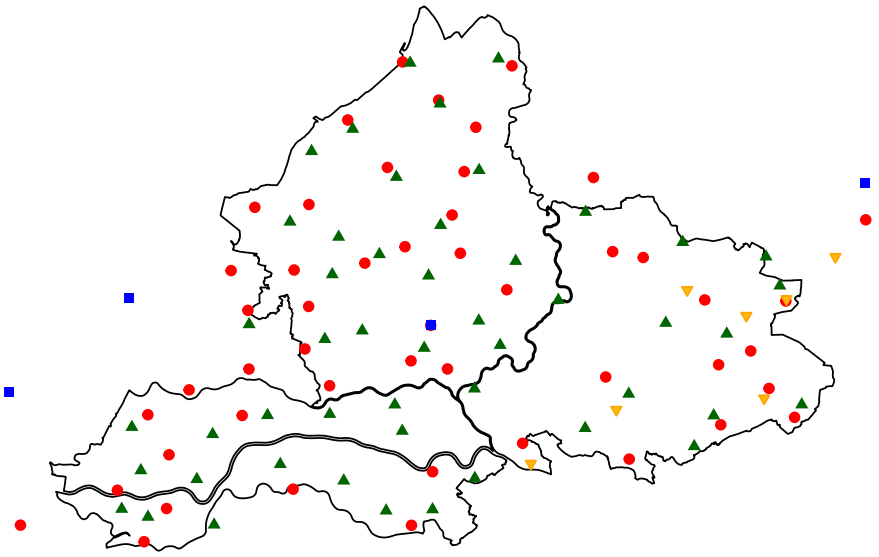

Figure 3.1: Locations of the 51 precipitation stations (red circles), locations of the 4 potential evaporation stations (blue squares), locations of the 7 runoff stations (orange triangles) and locations of the 49 piezometers (green triangles) situated in or close to the province of Gelderland (Dinoloket, 2014; KNMI, 2014).

3.1.2 Potential evaporation data

Under Dutch conditions, potential evaporation is well described by the Makkink equation. The Makkink reference evaporation is mainly driven by incoming shortwave radiation and temperature (Makkink, 1957; Buishand and Velds, 1980; Hiemstra and Sluiter, 2011):

$$ET_{ref} = C * \frac{s}{s+\gamma} * \frac{S^{\downarrow}_{day}}{\lambda * \rho} \tag{3.1}$$

where ET_{ref} is the Makkink reference evaporation (md^{-1}), C a constant equal to 0.65, *s* the slope of the curve of saturation water vapor pressure (kPa/ °C), γ the psychometric constant (kPa/ °C), $S^{\downarrow}_{day}$ the daily incoming shortwave radiation $(Jm^{-2}d^{-1})$, λ the heat of vaporization (JKg^{-1}) and the ρ the bulk density of water, i.e. 1000 kgm^{-3}.
The slope of the curve of saturation water vapor pressure is related to mean daily temperature:

$$s = \frac{7.5 * 237.3}{(237.3 + T_{day})^2} * ln10 * e_s \tag{3.2}$$

where e_s equals:

$$e_s = 0.6107 * 10^{\frac{7.5 * T_{day}}{237.3 + T_{day}}} \tag{3.3}$$

The psychometric constant (γ) is also related to T_{day}:

$$\gamma = 0.0646 + 0.00006 * T_{day} \tag{3.4}$$

The heat of vaporization (λ):

$$\lambda = (2501 - 2.375 * T_{day}) * 1000 \tag{3.5}$$

So only the T_{day} and $S^{\downarrow}_{day}$ are needed as input data for the calculation of reference evaporation. The KNMI measures the temperature at a height of 1,5 m above the surface and also measures the global radiation. On 35 KNMI stations the temperature and global radiation are measured continually and automatically, see Appendix A. Maps and data are available on `www.knmi.nl`. Time series of temperature (T_{day}) and global radiation ($S^{\downarrow}_{day}$) were downloaded from the KNMI website. Four stations were selected to cover the province of Gelderland namely Cabauw, De Bilt, Deelen and Twente (Figure 3.1). Two assumptions were made to calculate the Makkink reference evaporation, the γ was kept constant at 0.66 mbar/$^{\circ}$C and the λ was kept constant at 2.45$\times 10^6$ J/Kg. The Makkink reference evaporation is directly the potential evaporation based on the assumption that the crop-factor is 1. Finally inverse distance weighting was used to interpolate between the four stations. The interpolated potential evaporation field was used to calculate the values at the location of the precipitation stations (Figure 3.1).

3.1.3 Soil moisture data

Different satellite sensors measure soil moisture with differences in spatial, temporal and spectral resolution (Owe et al., 2008). Surface soil moisture was estimated from measurements taken by the ASCAT satellite (Huza et al., 2014). The ASCAT data give information on the saturation of soil moisture of the upper 2 cm with respect to the long-term average. The data have a spatial resolution of approximately 15 by 15 km, depending on the position of the satellite with respect to earth surface (Wanders et al., 2012). For this research the resolution was sufficient because the focus is on a regional scale in the province Gelderland. Longer time series were available from other satellites, but spatial resolution of this data was much lower. Therefore, these data were not used in this study.

3.1.4 Runoff data

A selection was made of rivers that start or flow for a large part through The Netherlands and have a year round discharge caused by a natural gradient in the landscape. The waterboards which are responsible for the maintenance provided discharge data. Table 3.1 gives an overview of the collected runoff data. The Rhine and Meuse were also taken into account because both rivers have some important branches in The Netherlands. In drought periods smaller brooks can be influenced by the use of inflow of river water and the discharge is not natural anymore. These brooks (Sallandse Weteringen) are not taken into account in

this study because the time series are not reliable. A description of all the catchments used in this research can be found in Appendix B.

3.1.5 Groundwater data

The data from a large number of piezometers is available via `www.dinoloket.nl`. The following two steps were taken to select piezometers from the database of DINOloket; 1) zoom in on the province of Gelderland; and 2) select a time period of at least 25 years. The location of a piezometer in a field, for example close to a road or water extraction area, can influence the quality of the data. The location was not a requirement for the selection of the data. In Table C.1 in Appendix C an overview is given of the piezometers used in this study.

3.2 Drought indices methods

3.2.1 KNMI index

In The Netherlands the commonly used deficit method is based on precipitation and potential evaporation. The KNMI records these data and publishes them each day on their website. The deficit is calculated by the difference between the precipitation and the potential evaporation starting on the 1st of April. The potential evaporation is calculated by the "reference crop-evaporation" which is determined by the method of Makkink (Buishand and Velds, 1980). The "reference crop-evaporation" can be multiplied by a crop factor which is described in tables depending on the crop (Hooghart and Lablans, 1988). The starting date is always 1 April, this is the first official day of the growing season (hydrological summer half year) and it ends on the last day of September when the autumn starts.

3.2.2 Standardised indices

The SPI, SPEI, SRI, SWI and the SMA are all based on the same concept. Central to all these indices is the standardised value, the so-called Z--value, which is calculated by:

$$Z = \frac{x_i - \mu_i}{\sigma} \tag{3.6}$$

where x_i is the variable, μ_i is the mean and σ the standard deviation. The use of Z-values requires the data to be normally distributed or transformation into normal distribution in case the distribution of the

Table 3.1: Overview of available discharge observations

River	Responsible waterboard	Data availability	Number of years with observed runoff	Number of missing days and remarks
Beerze	De Dommel	1-1-1977 till 17-7-2012	36	1700
Berkel	Rijn en IJssel	1-7-1971 till 16-5-2013	43	783
Bovenslinge	Rijn en IJssel	31-5-1972 till 16-5-2013	42	2868
Dommel	De Dommel	1-1-1978 till 4-7-2012	36	2431
Donge	Brabanste Delta	1-1-1995 till 12-5-2013	19	113
Essche stroom	De Dommel	1-1-1973 till 31-07-2007	35	342
Geelebeek	Regge en Dinkel	1-1-2000 till 16-11-2013	14	167
Geleenbeek	Roer en Overmaas	22-7-1971 till 23-5-2013	43	2630
Groenlosche Slinge	Rijn en IJssel	5-11-1976 till 29-11-2013	38	1439
Geul	Roer en Overmaas	3-9-1969 till 16-5-2013	45	1099
Hunze	Hunze en Aa's	1-1-2000 till 16-8-2012	13	0
Hupsel	Rijn en IJssel	1-1-1980 till 13-9-2013	34	1394
Meuse	Rijkswaterstaat	1-1-1911 till 31-12-2010	100	0
Nieuwe Leij	De Dommel	1-1-1980 till 1-8-2012	33	1090
Oude IJssel	Rijn en IJssel	30-11-1978 till 16-5-2013	36	2619
Regge	Regge en Dinkel	1-1-1995 till 31-12-2012	18	0
Reusel	De Dommel	1-1-1980 till 26-7-2012	33	2912
Roer	Roer en Overmaas	31-10-1969 till 16-5-2013	45	39
Rhine	Rijkswaterstaat	1-1-1901 till 31-12-2010	110	0
Schipbeek	Rijn en IJssel	1-1-1978 till 16-5-2013	36	2187
Springendalse-beek	Regge en Dinkel	1-1-1993 till 3-11-2013	22	445
Tongelreep	De Dommel	01-01-1976 till 31-7-2012	37	1710
Vecht (Overijssel)	Velt en Vecht	1-1-1996 till 29-5-2013	54	1516

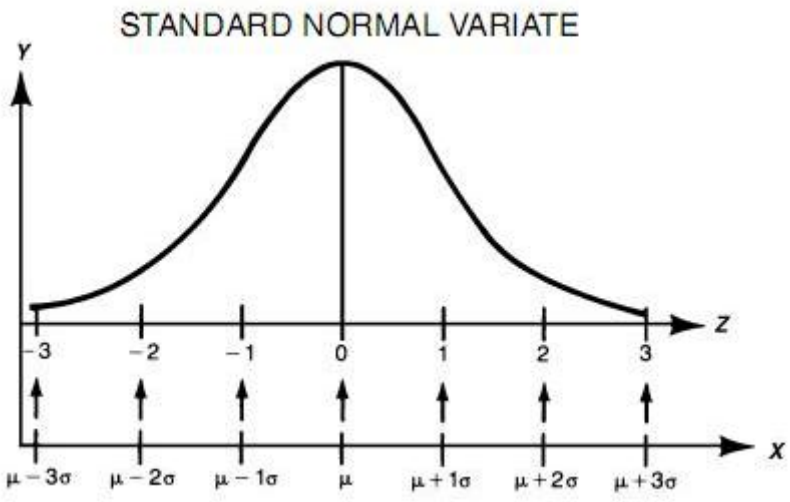

Figure 3.2: Comparison of Z-values to standard normal distribution (Lloyd-Hughes and Saunders, 2002).

Table 3.2: Drought categories for the SPI including probabilities (McKee et al., 1993)

Z-value	Drought category	Probability %
0 to −0.99	Normal conditions	34.1
−1.00 to −1.49	Moderate drought	9.2
−1.5 to −1.99	Severe drought	4.4
−2.00 or less	Extreme drought	2.3

original data is different. In Figure 3.2 is illustrated how the Z-values can be compared to a standard normal variate.

All the standardised indices are dimensionless and can be classified into a wet or dry category. Positive Z-values indicate higher than median precipitation (or other variables), while negative Z-values indicate below median precipitation (or other variables). The original classification is used in our research (Table 3.2). The calculation steps were applied on long-term records of monthly time series of precipitation, evaporation, soil moisture, groundwater and runoff of the period 1988--2013. The gamma distribution is defined by the probability density function (Lloyd-Hughes and Saunders, 2002; Sönmez et al., 2005):

$$g(x) = \frac{1}{\beta^{\alpha}\Gamma(\alpha)} x^{\alpha-1} e^{\frac{-x}{\beta}} \tag{3.7}$$

where $\alpha > 0$ is a shape parameter, $\beta > 0$ is a scale parameter and $x > 0$ is the amount of the chosen variable. Long-term records (x) are converted into log-normal values to calculate the statistic A with:

$$A = ln(\bar{x}) - \frac{\sum ln(x)}{N} \tag{3.8}$$

where N is the number of observations. The statistic A is used for the calculation of the shape and scale parameters of the gamma distribution:

$$\alpha = \frac{1 + \sqrt{1 + \frac{4A}{3}}}{4A} \qquad \beta = \frac{\bar{x}}{\alpha} \tag{3.9}$$

Integrating the probability density function with respect to x and inserting α and β gives the formula of the cumulative probability:

$$G(x) = \frac{\int_0^x x^{a-1} e^{\frac{-x}{\beta}} dx}{\beta^{\alpha} \Gamma(\alpha)} \tag{3.10}$$

Since the gamma function is undefined for $x = 0$ and $q = P(x = 0) > 0$ where $P(x = 0)$ is the probability of zero precipitation, the cumulative probability becomes as follow:

$$H(x) = q + (1 - q)G(x) \tag{3.11}$$

In Figure 3.3 the histogram and corresponding fit of a cumulative gamma probability function as calculated from monthly precipitation data of the Zaltbommel measurement station is shown as an example. After this step the distribution was transformed into a normalised distribution with mean zero and variance of one.

The SCI-package in R was used to calculate the standardised values (Stagge et al., 2013; Gudmundsson and Stagge, 2014). The gamma distribution was used for SPI, SRI, SMA, SWI and the genlog distribution was used for SPEI. For the interpretation of all standardised indices Table 3.2 was used.

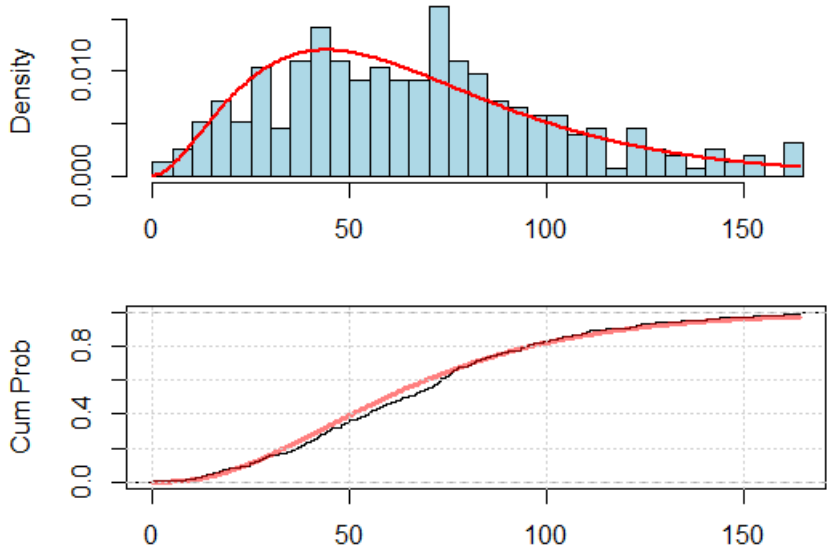

Figure 3.3: Example of a histogram as calculated from montly precipitation data of the Zaltbommel measurement station and the best fitting parametric distribution, for this example the gamma distribution.

Standardised precipitation index

A variety of time scales were calculated for the SPI, for example the 3-month SPI. This accumulation period compares the precipitation over a specific 3-month period with the precipitation totals from the same 3-month period for all the years in the observed record. For the other indices the same way of interpretation can be used.

Standardised precipitation evaporation index

With the interpolated potential evaporation values the SPEI values of the 51 precipitations stations were calculated. This was done by subtracting the potential evaporation values from the precipitation values. For SPEI a different distribution should be applied as the SPI because negative values are included in SPEI. In this research the genlog distribution was chosen because this distribution can handle negative values.

Standardised runoff index

An important remark regarding SRI is that a lot of gaps were present in the discharge data. The months in which these gaps occurred were not taken into account in order to get a better and more reliable result. For the temporal analysis only the runoff stations in or close to Gelderland were selected (Figure 3.1).

Standardised water level index

Since groundwater level is measured down from the surface, positive anomalies correspond to drought and negative anomalies to no drought. So all the SWI values are multiplied with minus one in order to compare them with the other variables.

Soil moisture anomalies

In order to test if soil moisture would need transformation a QQ-plot was made to investigate whether the data follow a normal distribution. The middle grid cell in the province of Gelderland was selected as being representative. In Figure 3.4 an example is given of the January months. Most Z-values of the January months closely align with the 1:1 line. Similar results of QQ-plots for other months can be found in Figure D.1 in Appendix D. Based on these plots we decided to use the normalised soil moisture observations without any transformation.

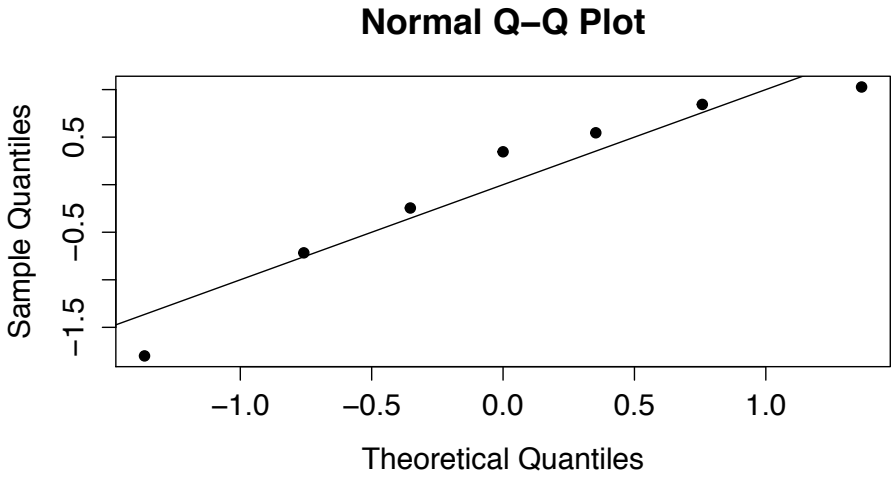

Figure 3.4: QQ-plot of all the January months from 2007 till 2013, in total seven January months.

3.2.3 Low flow indices

Base flow index

The base flow index was calculated by the ratio of base flow to the total flow from a hydrograph smoothing and separation procedure using daily discharges (Section 3.1.4). The R-package "lfstat" was used for the calculation of all the mentioned low flow indices in this study.

Mean annual minimum flow

The mean annual minimum flow was derived from a series of annual minima of n-day average flow. First the moving average values were calculated of the last 1-day, 3-days, 7-days and 30-days of the period 1988--2013. Then the annual minimum values were selected and the average of the annual minimum was calculated (Tallaksen and Van Lanen, 2004).

Percentiles from the flow duration curve

The flow duration curve plots are the empirical cumulative frequency of streamflow as a function of the percentage of time when the streamflow is exceeded. Low flow indices were derived directly from the

curve as low-flow exceedances. Q70, Q90 and Q95 are chosen and lie within the 70th -- 95th percentile range which is commonly used in drought studies (Van Loon and Van Lanen, 2012).

Threshold level

In this study a fixed and variable threshold were used. In Figure 3.5 we see an example of a discharge serie with a fixed and variable threshold. The difference between both thresholds is that the variable threshold takes the seasonal variation into account (Van Loon and Van Lanen, 2012). The area between the threshold line and the time series indicates the drought deficit volume. A 90th percentile threshold was chosen to see the impact of more severe droughts in The Netherlands. The variable threshold was calculated based on a 30 days moving window (Beyene et al., 2014).

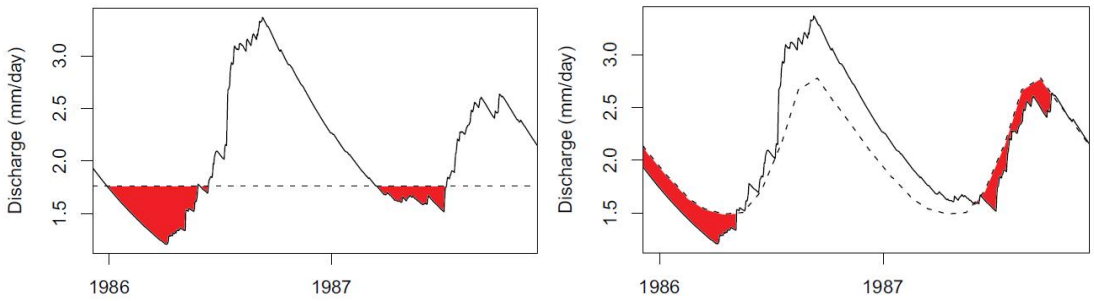

Figure 3.5: Example of a discharge serie with a fixed threshold (left) and a variable threshold (right) (Wanders et al., 2012).

3.3 Statistical analyses

Correlation between two variables was tested with the correlation coefficient. The coefficient ranges between -1 and 1, -1 indicates a strong inverse relationship, 0 indicates no relationship and +1 indicates a strong direct linear relationship (Kendall and Alan, 1961). To test significant correlation between the variables with different time scales, the *Pearson* test was used. The correlation coefficient is called statistically significant if in this test the probability is lower than the conventional 5% ($P < 0.05$) (Kendall and Alan, 1961). SRI was not taken into account due to the limited spatial coverage. SMA was not used due to the short period of the available data. Two statistical correlations were performed:

1. In order to statistically compare the SGI, SPI, SPEI and KNMI index the same x and y coordinates of these indices were selected. The interpolated fields of SPI, SPEI and KNMI maps were used to determine the interpolated values on the locations of the groundwater observations wells. The 6-month SPI, 6-month SPEI, KNMI index and 1-month SGI of the September months were selected to calculate the correlation.

2. The 1-month SGI was correlated with the locations of the groundwater observation wells in the interpolated fields of 1-, 3-, 6-, 9-, 12-, 24-month SPI. The correlation coefficients were significantly

tested by the *Pearson* test.

3.4 Spatial interpolation methods

Point values of the individual stations of the SPI, SPEI, SRI, SMA and SWI have been interpolated to generate maps for the province of Gelderland. Several different interpolation techniques exist, see Longley (2005). An important aspect of interpolation is that the quality of any applied analysis that relies on interpolation is subject to a degree of uncertainty. To obtain a gridded map, each grid node gets an interpolation estimate. Three different interpolation methods were applied, which are described in the following sections. The input map for the interpolation is a shape file of the province Gelderland in Rijksdriehoeksmeting coordinates. For visualisation only the boundaries of the province of Gelderland are used.

3.4.1 Inverse distance weighted

Inverse distance weighted (IDW) interpolation uses the measured values surrounding the prediction location. IDW gives greater weights to points closest to the prediction location, and the weights diminish as a function of distance. A commonly used function is written by Shepard (1968). The method uses a weighted average by distance to a data point. The function is:

$$u(x) = \frac{\sum_{k=0}^{N} W_k(x) u_k}{\sum_{k=0}^{N} W_k(x)} \tag{3.12}$$

where W_k(x) equals:

$$W_k(x) = \frac{1}{d(x, x_k)^p} \tag{3.13}$$

where x is the interpolated point, x_k are the known data points of which there are N in total, u is the value at both the interpolated and the know data points, $d(x, x_k)$ stands for the distance between the interpolated point x and known point x_k and p is the power parameter. Larger p values give bigger influence to the data points nearby the interpolated point. The interpolated field was filled grid cell by grid cell and finally clipped to the shape of the province of Gelderland. IDW has a local pattern, which means that local differences between stations are well visible.

3.4.2 Ordinary kriging

The best known geostatistic approach for interpolation is kriging. Many different methods are related to kriging. In this research so-called *ordinary* kriging is used. First a semivariogram of the predictability of the known values is calculated. The method relies on the semivariogram to measure the expected similarity between observations in space:

$$\gamma(h) = \frac{1}{2n}\sum_{i=1}^{n}[Z(x_i) - Z(x_i + h)]^2 \tag{3.14}$$

where n is the number of pairs of data point, separated by h distance, $Z(x_i)$ and $Z(x_i + h)$ are the values of the variable Z at x_i and $x_i + h$ locations (Goovaerts, 1997). To estimate the values at unknown locations a mathematical function is fitted to the semivariogram, the variogram model. Semivariance is a measure of the degree of spatial dependence between samples. The coefficients of a variogram model are the nugget, sill and range. The nugget is the short scale variation and is the point where the variogram model crosses the y-axis. The sill is the maximum semivariance of the variogram model. The range is the value where the variogram model reaches the sill, beyond this point no spatial correlation is present anymore. With the variogram model and the trend coefficients the unknown locations can be estimated. All the calculated interpolation values were saved into a field to create a map.

3.4.3 Thiessen Polygons

When Thiessen Polygons are used for interpolation, an interpolated field consists of polygons with boundaries at a distance halfway between the stations. Lines are drawn between the measurement stations and subsequently perpendicular bisectors are drawn to create the Thiessen polygons. The procedure was run using Voronoi polygons with a point coverage of the selected measurement stations. More information on Voronoi polygons can be found in Okabe et al. (2009).

3.4.4 Comparison of the study area

The different interpolation techniques gave different outputs. The most coarse interpolation technique is Thiessen Polygons because there is no smooth gradient and the values only differ when the boundary of the polygon is crossed, an example is shown in Figure E.1 of Appendix E. This technique assumed not to be representative and was therefore not used in the remainder of this study. To apply *ordinairy* kriging a semivariogram was needed. A nugget, range and sill need to be fitted and thus need to be identifiable

in order to fit the semivariogram. When applying kriging for every variable and time scale a separate fit was needed which was quite time consuming. For groundwater time series the variogram model could not be fitted (Figure E.2 in Appendix E). The inversed distance weighting technique needed less assumptions. Only one parameter, the power parameter with a value of 2, was chosen. The interpolated maps of both techniques showed quite similar results (Figure E.3 to E.6 in Appendix E). For the SPI, SPEI, SMA, SWI and KNMI maps inversed distance weighting was chosen as interpolation technique. Runoff data were not used for spatial analysis due to limited spatial coverage and short length of the available data.

4 Results

Historic drought events are investigated in Chapter 4 with the methods described in Chapter 3. In Section 4.1 the historic perspective and a general drought overview is described for the period from January 1988 to September 2013. After that, two selected severe drought events are highlighted: the year 1996 and summer 2003. Section 4.2 continues with the spatial distribution of the selected droughts events. In Section 4.3 the correlation between some of the indices is discussed and finally in Section 4.4 the space-time variability in runoff drought is explained.

4.1 Temporal evolution of drought in The Netherlands and Gelderland

4.1.1 Historic perspective

A period of 100 years, from 1911 to 2010, was chosen to see how the SPI and the SRI show corresponding results in dry and wet years in The Netherlands. The 12-month SPI of the meteorological stations De Bilt and Winterswijk and the 12-month SRI of the discharge stations Meuse and Rhine are illustrated in Figure 4.1 (both stations are close to the German and Belgian border).

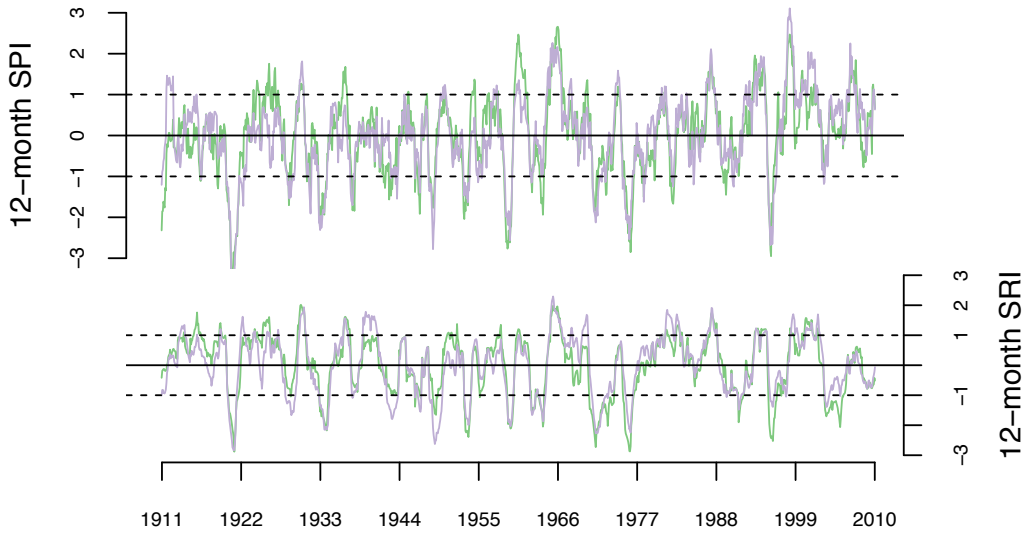

Figure 4.1: 12-month SPI Winterswijk (green) and De Bilt (purple) and 12-month SRI Meuse (green) and Rhine (purple).

By comparing the correlation coefficients of the SPI and SRI we see that the highest correlation is between the stations which measure the same variable, so between the two precipitation stations and between the two discharge stations (Table 4.1). In Figure 4.2 we see the cross-correlation (an estimate of the degree of which two series are correlated) of the discharge of the Rhine versus precipitation of De Bilt (left) and discharge of the Meuse versus precipitation of De Bilt (right). The time-lag in the left figure is higher than in

the right figure, which means that the precipitation of n days (lags) ago still influences the discharge. The higher amount of lags for the Rhine can be explained by the fact that the catchment of the Rhine is larger. Furthermore, the Rhine is a glacier-fed river, whereas the Meuse is only rain fed (although in winter and spring there can also be snow melt).

Table 4.1: Correlation between the SPI of the meteorological stations De Bilt and Winterswijk and the SRI of the rivers Rhine and Meuse

	de Bilt	Winterswijk	Rhine	Meuse
de Bilt	-	-	-	-
Winterswijk	0.86	-	-	-
Rhine	0.60	0.64	-	-
Meuse	0.64	0.68	0.88	-

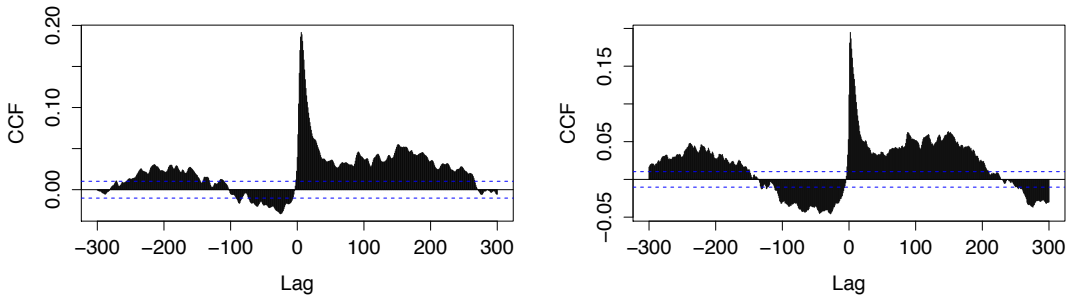

Figure 4.2: Cross-correlation series of the discharge of the Rhine versus precipitation of De Bilt (left) and discharge of the Meuse versus precipitation of De Bilt (right).

4.1.2 General overview 1988-2013

Based on the different variables (all except soil moisture, which is taken into account in next section) we could quantify relations between meteorological and hydrological drought. The drought indices clearly show the same major drought events (Figure 4.3 and 4.4). The black line indicates the average of the selected stations, the blue lines indicate the standardised values of the individual stations. Values between 1 and -1 correspond to normal conditions. Since the focus of this thesis is on dry conditions, no attention is given to positive values. The drought indices based on precipitation and potential evaporation are more variable with short extreme droughts alternated by short wet periods, while the drought indices based on discharge and groundwater have a smoothed signal. When comparing the indices for the individual stations with the average of Gelderland we found that the meteorological drought stations behave similarly, whereas especially the groundwater stations have markedly different responses to the same drought event. Furthermore, a delay from precipitation deficit towards drought in groundwater is visible. Prolonged drought periods are visible when a long time scale is used, Figure 4.4 compared to Figure 4.3. To zoom in, better understand and interpret specific drought a selection of the most significant droughts is chosen,

namely the 1995 - 1996 drought (clearly visible) and the 2003 drought (which affected most of western and central Europe).

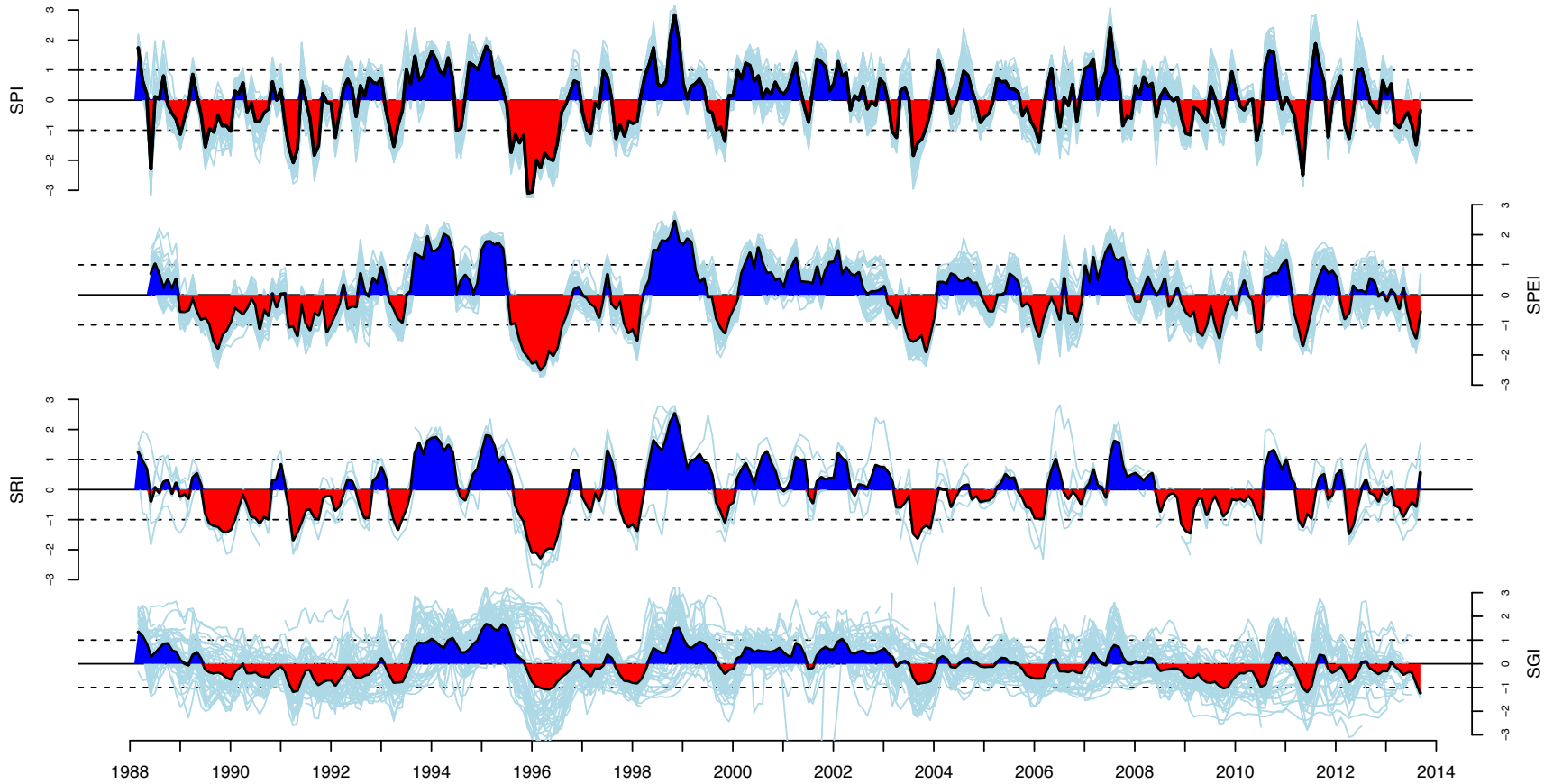

Figure 4.3: The 3-month SPI, SPEI, SRI and SGI of the time series 1988-2013. The black line is the average of the stations. The blue lines represent the individual calculated values of every stations. The dotted lines indicate the border of moderate dry/wet versus normal conditions.

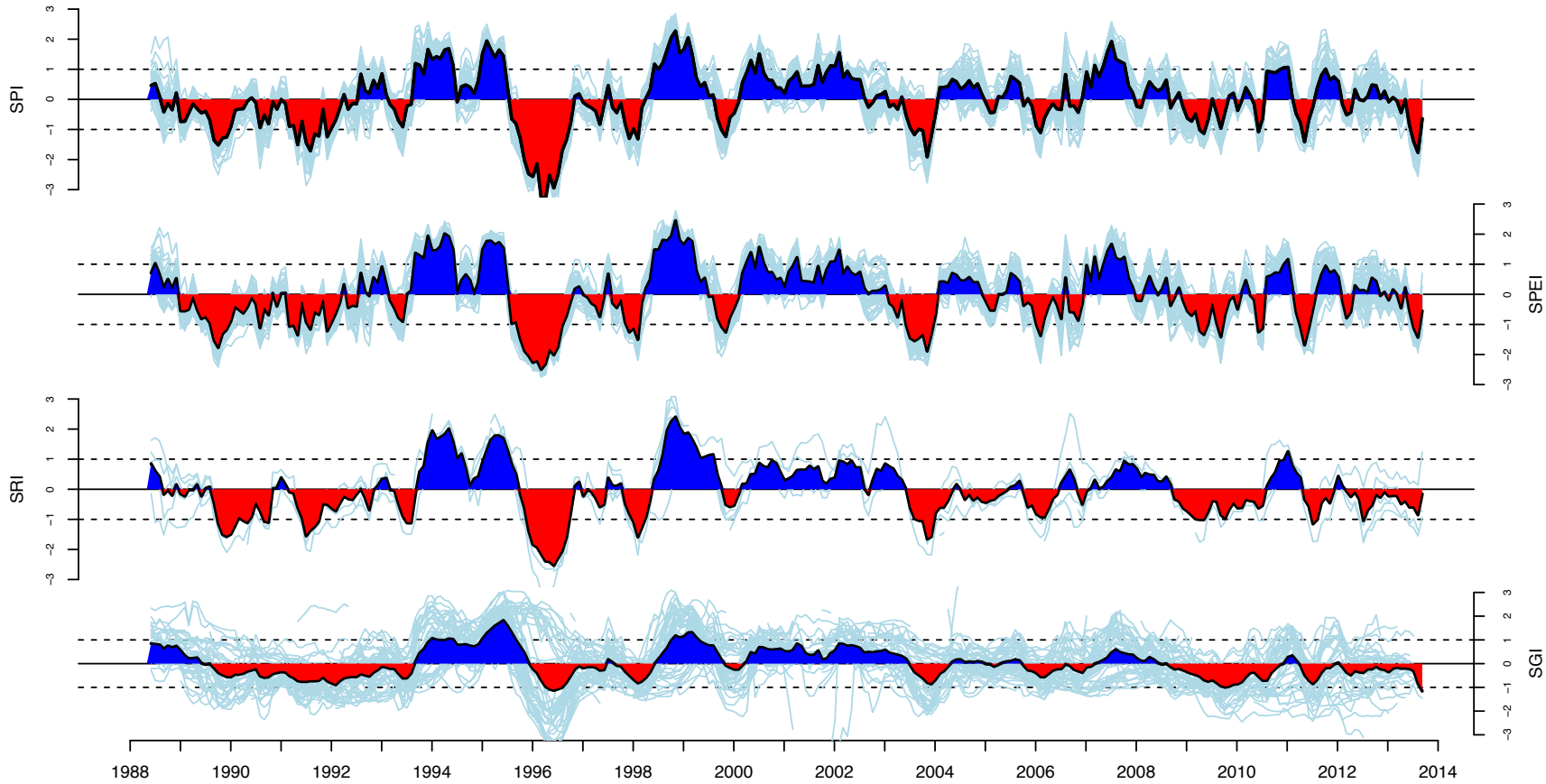

Figure 4.4: The 6-month SPI, SPEI, SRI and SGI of the time series 1988-2013. The black line is the average of the stations. The blue lines represent the individual calculated values of every stations. The dotted lines indicate the border of moderate dry/wet versus normal conditions.

4.1.3 Overview 2007-2013 with soil moisture

Time series of soil moisture are shorter compared to the other variables. To include soil moisture a comparison is made of the longest possible period, namely 2007--2013. The drought indices based on precipitation, potential evaporation and soil moisture are more variable in time, while indices based on discharge and groundwater have a smoothed signal (Figure 4.5). This signal is comparable with Figure 4.3 and Figure 4.4. In the previous section is shown that the indices for individuals stations of meteorological drought behave similarly. Now some of the individual stations of SPEI have extreme peaks in the short time series which is not visible in the SPI graph. This is caused by the short selected time series in combination with the extreme range in values. At the start of SMA a lot of grid cells show a deviation from the general trend. One special event to mention is the spring of 2007, where the drought category changes from extreme drought in SPI and SPEI to no drought conditions in the SGI graph looking at the average value.

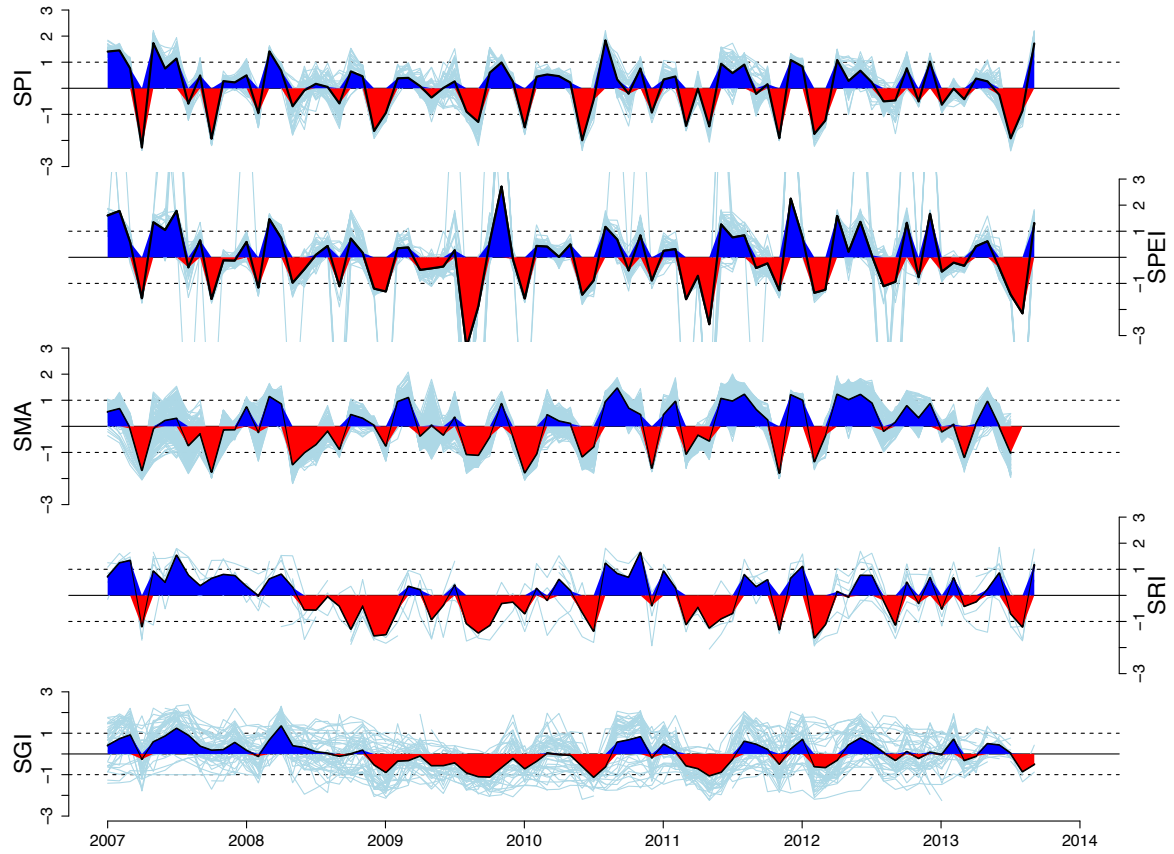

Figure 4.5: The 1-month SPI, SPEI, SRI, SSMI and SGI of the time series 2007-2014. The black line is the average of the stations. The blue lines represent the individual calculated values of every stations. The dotted lines indicate the border of moderate dry/wet versus normal conditions.

4.1.4 1995-1997 drought

The period 1995-1996 is one the most severe drought episodes in the observations (Figure 4.3 and Figure 4.4). From a drought in SPI to SGI, a delay of a few months can be identified (Figure 4.6). SPI and SPEI

experience drought conditions from August 1995 onwards whereas the SRI and SGI experience drought conditions from December 1995 and February 1996, respectively. So a delay from the meteorological to the hydrological drought is present, consistent with the hypothesis of Changnon (Figure 2.2). The severity of the drought differs significantly, SPI is on average −2.5 whereas the drought in SGI is slightly below −1. A remark is that the standard deviation of SGI is high compared with the other indices which means that the individual groundwater observation wells have different responses to the same drought event. Small standard deviations indicates that the individual stations behave similarly. Other accumulation periods in Figure F.1 in Appendix F and Figure G.1 in Appendix G.

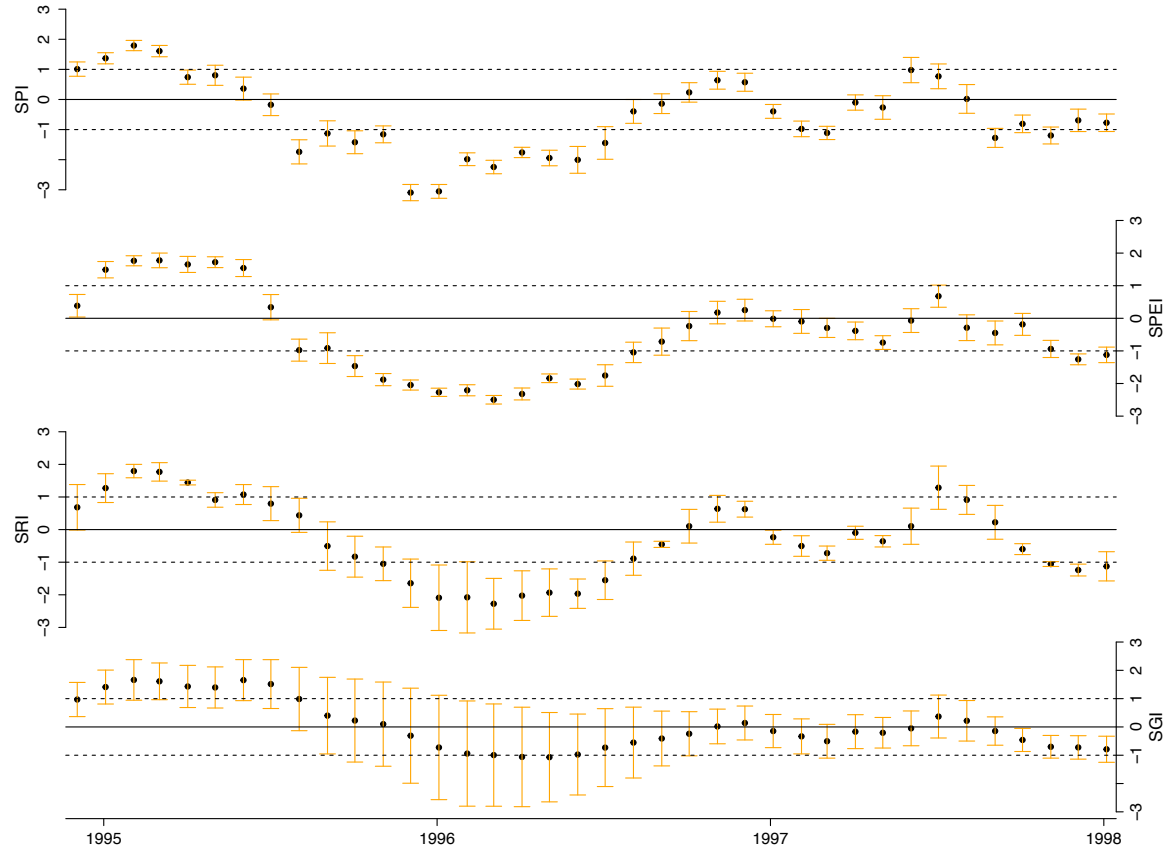

Figure 4.6: The 3-month SPI, SPEI, SRI and SGI for 1995-1997 with error bars. The error bars represent the spatial standard deviation of every month.

4.1.5 2003 Summer drought

In 2003, much of Europe suffered from very dry conditions (Fink et al., 2004; Marsh, 2004; Rebetez et al., 2006). The year 2004 is included to see how long it will take before the indices are recovered from drought conditions. Already after 1 month the SPI and SPEI stations experience no drought conditions anymore, whereas the recovery of SRI and SGI lasts for 2 till 3 months (Figure 4.7). The meteorological drought starts and ends earlier compared with the indices of the hydrological drought. The meteorological drought shows two drought periods in 2003: the first drought is during spring (March and April) and the second drought is during the end of summer and start of autumn (August to November). The SRI experience

drought conditions during this second period. No drought in groundwater is visible, only several individual groundwater observation wells experience moderate drought conditions. Other accumulation periods in Figure F.2 in Appendix F and Figure G.2 in Appendix G.

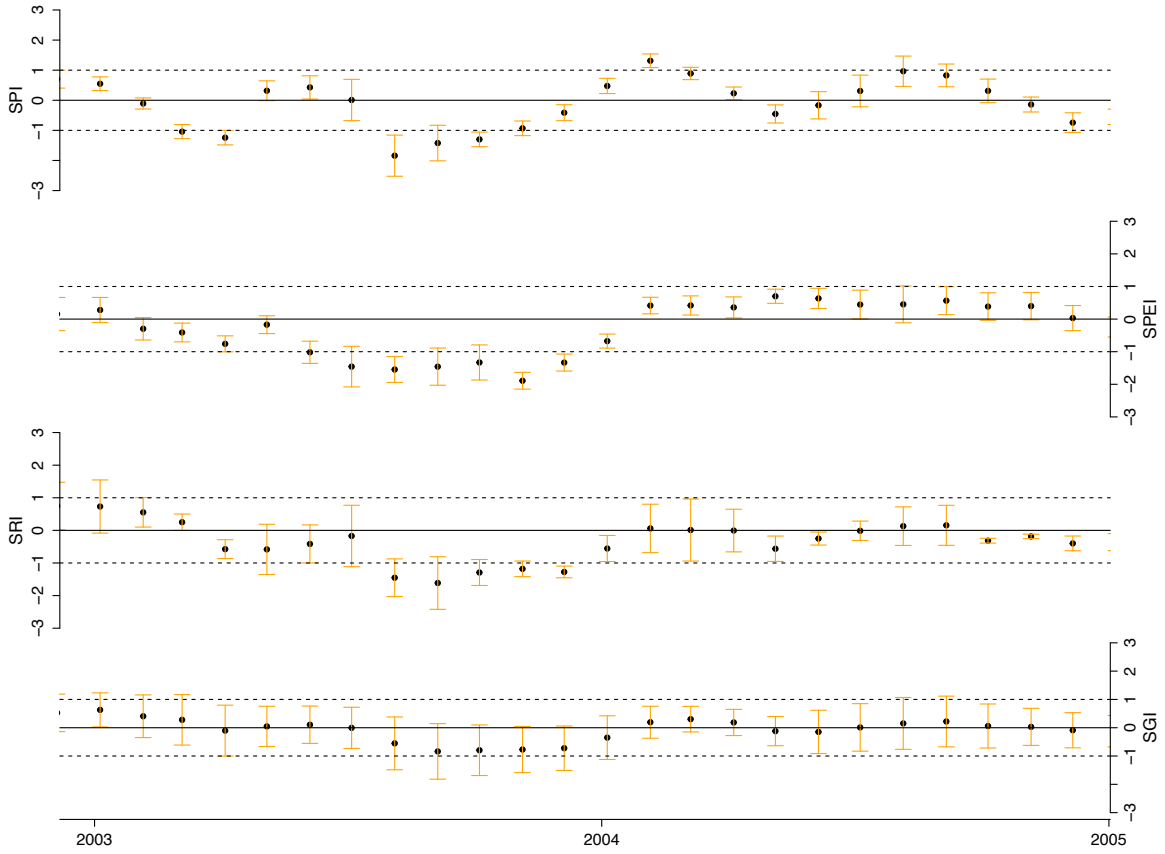

Figure 4.7: The 3-month SPI, SPEI, SRI and SGI for 2003-2004 with error bars. The error bars represent the spatial standard deviation of every month.

4.2 Spatial distribution drought indices

Interpolated maps of SPI, SPEI, SGI and KNMI are compared to quantify drought conditions in Gelderland. The quantification of runoff droughts is described in Section 4.4.

12-month -- August 1996

In Figure 4.8 we see the 12-month interpolated maps for August 1996, the accumulation period of September 1995 to August 1996 is covered. The exception is the map of the KNMI, which only covers the period April 1996 to August 1996. The implicit assumption behind the KNMI index is that there are significant precipitation amounts during the winter and replenishment of recharge to the groundwater. This is not the case in the winter 1995 -- 1996. Based on the KNMI map, the highest deficits are in the western part. The spatial distribution of meteorological drought is uniform over Gelderland, whereas large spatial variations exist in the hydrological drought. In areas with shallow groundwater tables (Figure 2.7) severe hydrological

drought conditions are present in contrast to areas with deep groundwater tables where still wet conditions are present.

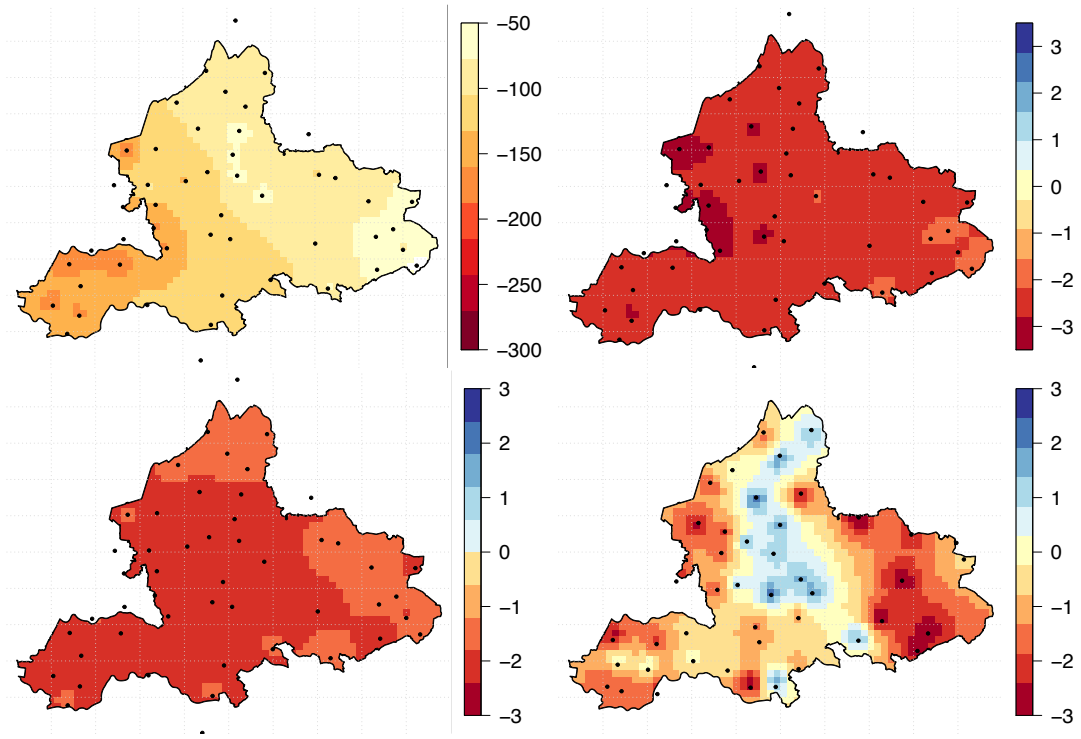

Figure 4.8: The KNMI map (upper-left) unit is mm, the 12-month SPI (upper-right), 12-month SPEI (lower-left) and 12-month SGI (lower-right) for August 1996.

1-month -- August 2003

August is the driest month during 2003. The 1-month SPI and SPEI maps of August 2003 show a uniform pattern, the southern part in the SPI map experience no drought conditions (Figure 4.9). In the SGI map regional differences are observed between the higher situated parts compared to the lower situated parts of Gelderland.

6-month -- September 2003

The 6-month SPI and SPEI maps of September 2003 show that the western and north-western area of Gelderland were dryer compared to the eastern area of Gelderland. The map of the KNMI also shows the same difference between the western and eastern areas of Gelderland. The SGI-maps again show regional differences between *Veluwe* and *Betuwe* (Figure 4.10).

1-month -- May 2011

In the SPI and SPEI maps of May 2011 the values are in the same range and the drought covers most of Gelderland (Figure 4.11). The SMA map shows moderate to normal conditions. The SGI map has wet and extremely dry conditions relatively close to each other. One well shows a positive value, indicating wet conditions.

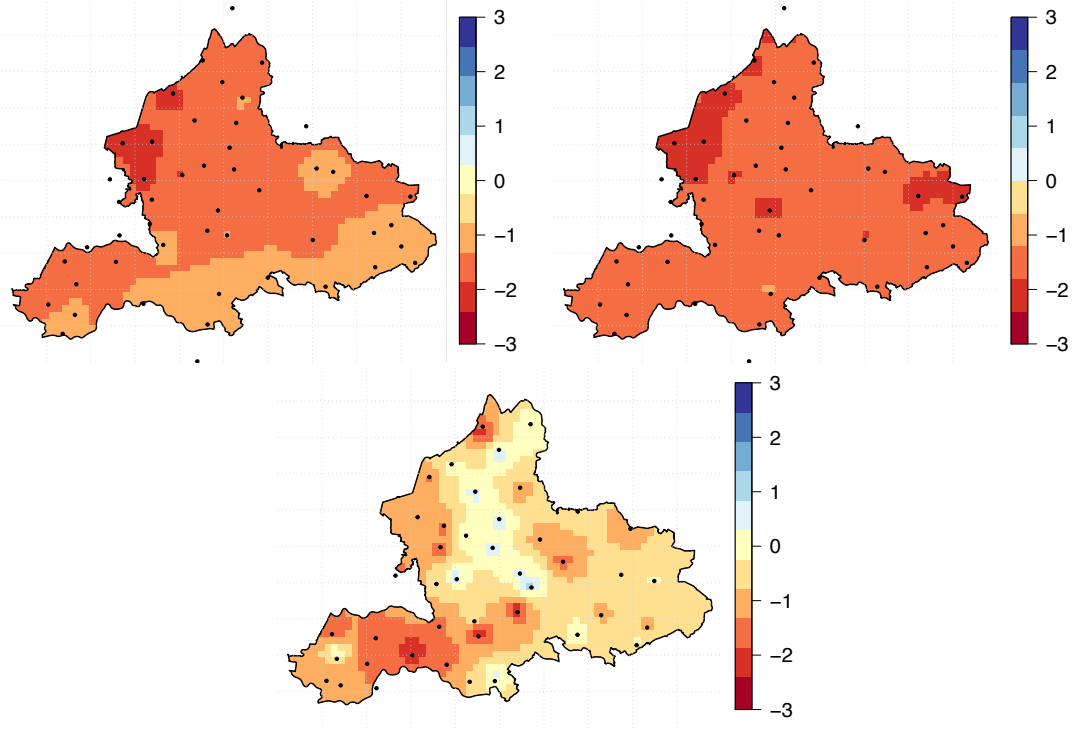

Figure 4.9: The 1-month SPI (upper-left), 1-month SPEI (upper-right) and 1-month SGI (lower-middle) for August 2003.

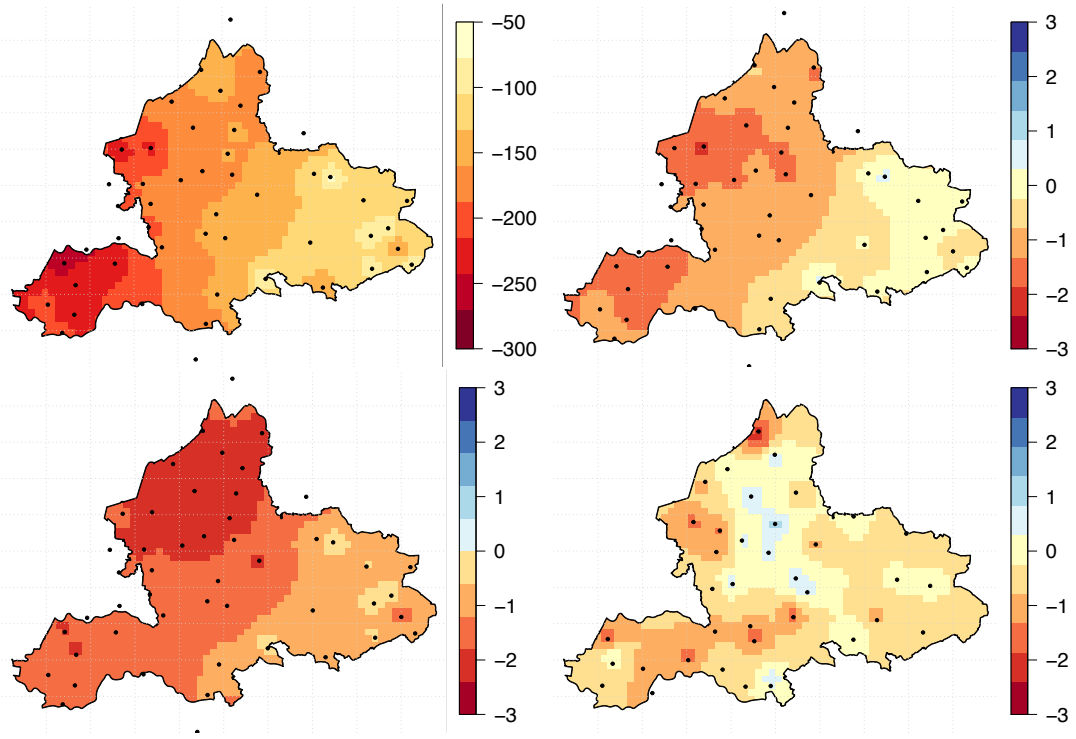

Figure 4.10: The KNMI map (upper-left) unit is mm, the 6-month SPI (upper-right), 6-month SPEI (lower-left) and 6-month SGI (lower-right) for September 2003.

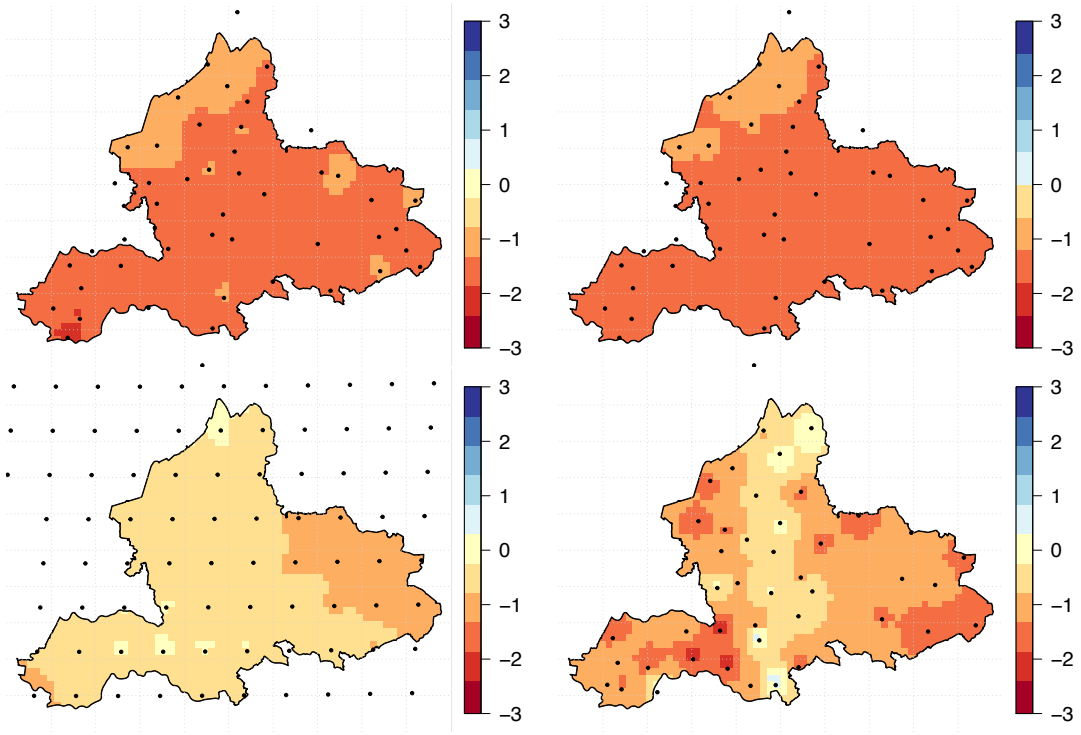

Figure 4.11: The 1-month SPI (upper-left), 1-month SPEI (upper-right), SMA (lower-left) and 1-month SGI (lower-right) for May 2011.

4.3 Correlation between the indices

The SPI accumulation period with the highest correlation between 1-month SGI and SPI is shown for the period 1988--2013 (Figure 4.12). The wells on the *Veluwe*, *Berg en Dal* and *Montferland* have the highest correlation with 24-month SPI. The wells situated in the *Betuwe* and the *Achterhoek* have the highest correlation with 1-,3- and 6-month SPI. All correlation coefficients are proved significantly by Pearson test. 9-month SPI has nowhere the highest correlation.

In Figure 4.13 we see the mean and standard deviation of the 6-month KNMI of the September months versus the 1-month SGI of the September months and the 6-month SPEI of the September months respectively. The scatter in 1-month SGI is higher than the scatter in the 6-month KNMI. A very small scatter exists between the 6-month KNMI versus 6-month SPEI because both are using the same input time series. In Appendix G the plots with KNMI -- 6-month SPI, 6-month SPI -- 6-month SPEI, 6-month SPI -- 1-month SGI, 6-month SPEI -- 1-month SGI are shown. For meteorological indices the standard deviations are smaller and 1:1 correlation is high.

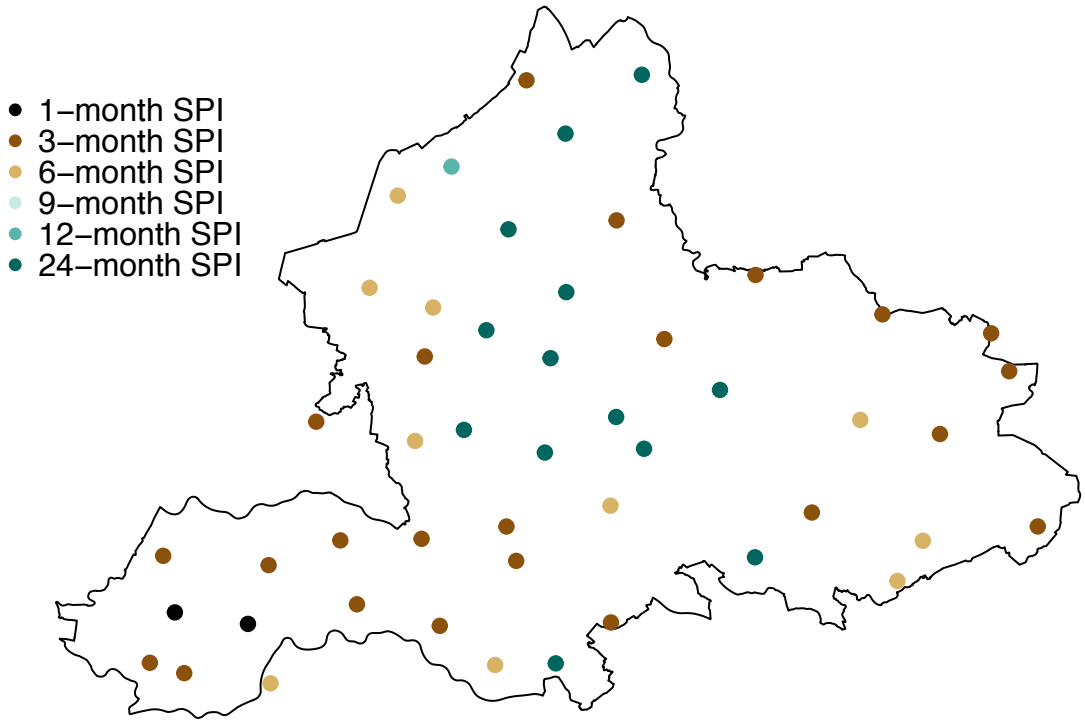

Figure 4.12: Highest correlation between the SPI accumulation period versus 1-month SGI.

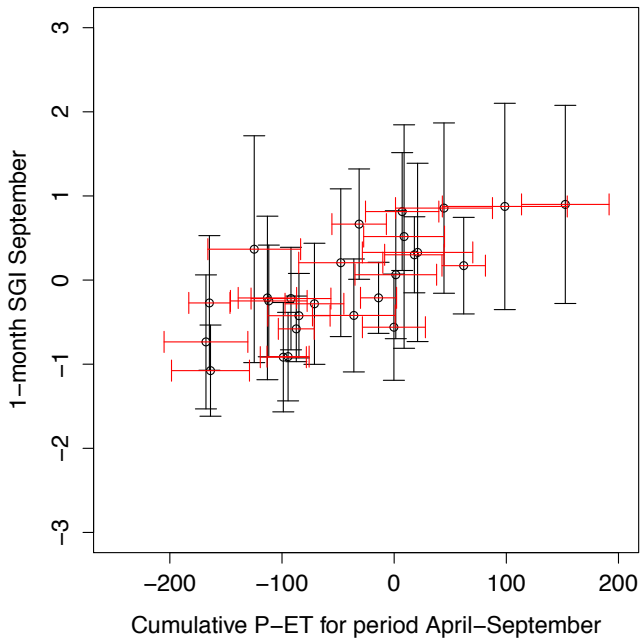

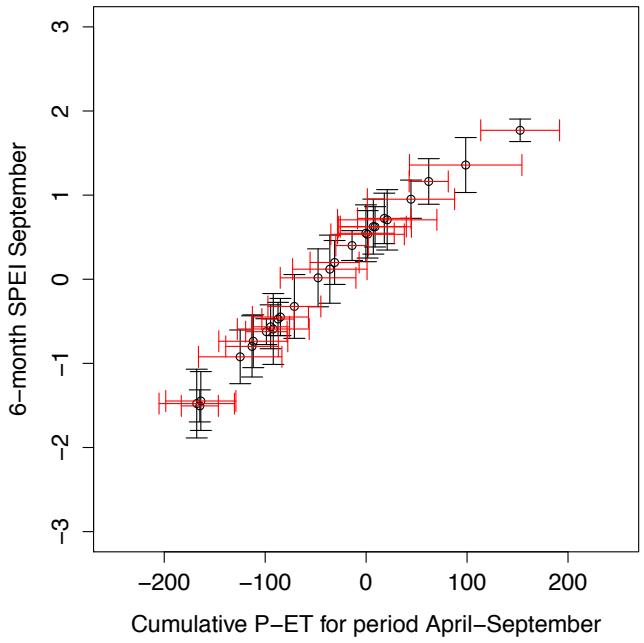

Figure 4.13: Mean and standard deviation of cumulative precipitation minus evaporation of the period April till September versus 1-month SGI of the September months (top) and 6-month SPEI of the September months (bottom).

4.4 Space-time variability runoff

Runoff measurements were not useful for spatial analysis of drought due to limited spatial coverage and short length of available data. In order to quantify drought and low flow in runoff data low flow indices were applied.

4.4.1 Low flow indices

In Table 4.2 we see a selection of low flow indices for three rivers (the other low flow indices can be found in Table I.1 in Appendix I). The general trend is an increase in MAM values with increasing window because a larger window for moving average results in a higher annual minimum. The transition from Q70 to Q90 is relative large which is related to the shape of the FDC. The catchment areas of the rivers differ significantly, i.e. the *Meuse* catchment area is 35000 km^2, the *Rhine* catchment area is 170000 km^2, whereas the Hupsel has a catchment size of only 6.5 km^2. A larger catchment results in higher low flow indices. The size of the catchment is recognised in the BFI values of the *Meuse* (0.53), *Rhine* (0.83) and *Hupsel* (0.40). The *Rhine* has the highest contribution of groundwater and other delayed sources (shallow subsurface storage, melt-water from glaciers) to the river flow.

Table 4.2: Overview of low flow indices for the selected rivers

	Meanflow $[\frac{m^3}{s}]$	MAM1 $[\frac{m^3}{s}]$	MAM3 $[\frac{m^3}{s}]$	MAM7 $[\frac{m^3}{s}]$	MAM30 $[\frac{m^3}{s}]$	Q70 $[\frac{m^3}{s}]$	Q90 $[\frac{m^3}{s}]$	Q95 $[\frac{m^3}{s}]$	BFI
Hupsel	6.3×10^{-2}	2×10^{-3}	2.2×10^{-3}	2.5×10^{-3}	4.1×10^{-3}	7.9×10^{-3}	3×10^{-3}	2×10^{-3}	0.397
Meuse	230	9.03	11.2	15.3	23.5	58	16	10.1	0.541
Rhine	2215	1075	1084	1106	1242	1548	1221	1102	0.834

4.4.2 Fixed and variable threshold

When a variable threshold is used we see that the mean duration, mean deficit and number of drought are higher (Table 4.3). For the *Hupsel* and the *Rhine* the mean duration is smaller for the variable threshold compared to the fixed threshold . The results of the other rivers can be found in Table I.2 in Appendix I.

Table 4.3: Drought characteristics using a 90 percent fixed and variable threshold

		Mean duration [days]	Mean deficit $[\frac{m^3}{s}]$	No. of drought events
Hupsel	Fixed	9.44	9.39×10^{-3}	80
	Variable	8.47	7.4×10^{-2}	229
Meuse	Fixed	3.24	17	256
	Variable	4.68	118.7	410
Rhine	Fixed	14.68	2117	57
	Variable	13.56	2504	116

4.4.3 Spatial distribution of drought

In Figure 4.14 we see the SRI for the selected runoff stations. The catchment characteristics (land-use, soil type, slope, etc.) determine how quick or slow a catchment reacts to a precipitation deficit. For every applied catchment these characteristics are unique and therefore regional differences are visible in both maps, from extreme to normal drought conditions.

The *Dommel* contains two measurement locations, one upstream and one downstream. This provides an opportunity to see if a specific drought influences the whole river. In the end of the time series gaps are present which influence the quality of the data (Figure 4.15). The correlation coefficients are from top to bottom are respectively 0.85 (1-month SRI), 0.87 (3-month SRI), 0.89 (6-month SRI) and 0.91 (9-month SRI). This indicates that both locations are influenced at the same time, so drought affects the whole catchment at the same time. When the time scales are larger the correlation coefficient also increases because the line becomes more smoothed. Both the *Schipbeek* and the *Groenlosche Slinge* also contain two measurement locations, but due to a significant amount of gaps in the time series the same analysis could not be done on those rivers.

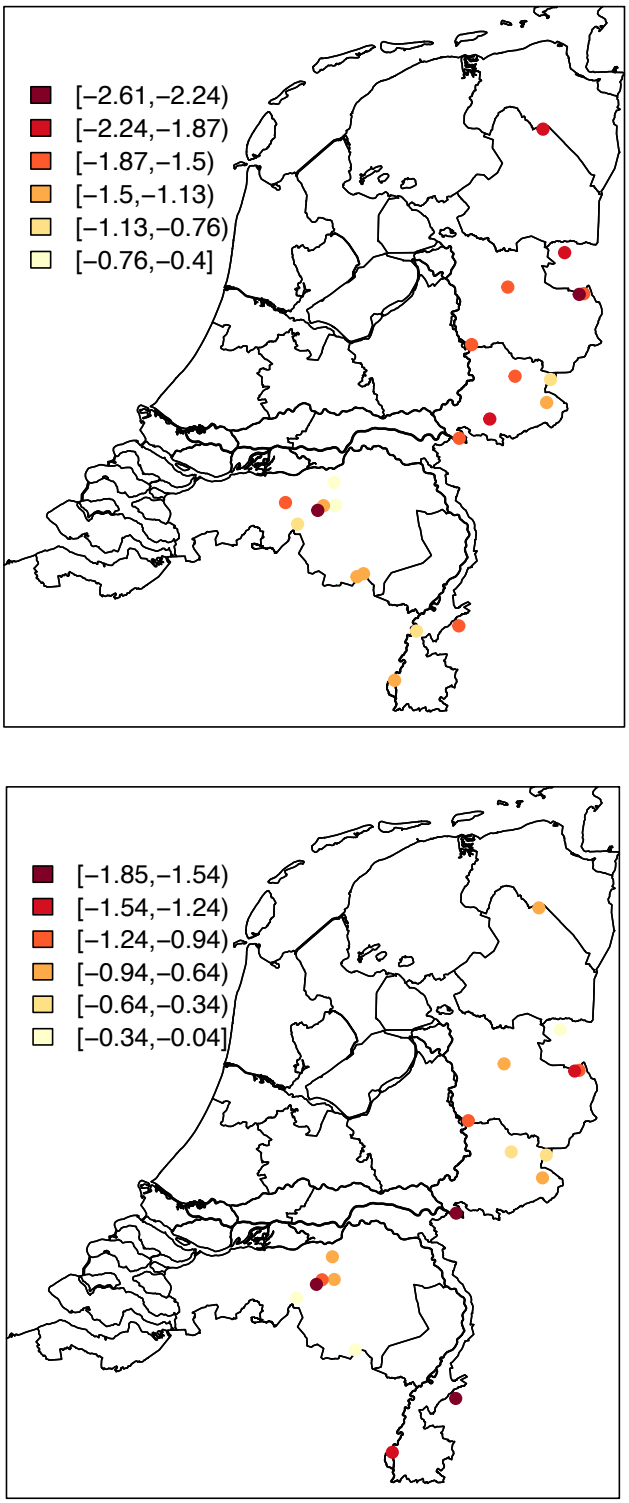

Figure 4.14: The 1-month SRI of August 2003 (top) and 6-month SRI of September 2003 (bottom) based on measured runoff.

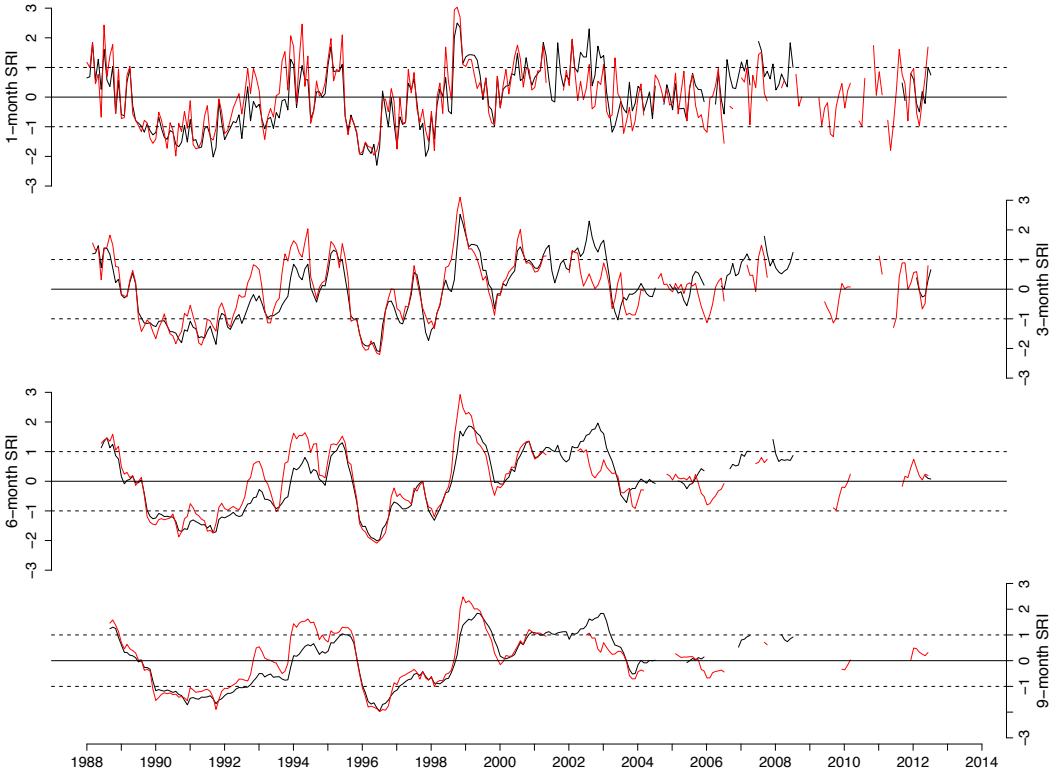

Figure 4.15: The upstream and downstream location of river the *Dommel* of the 1-, 3-, 6- and 9-month SRI. Black line indicates the upstream *Dommel* and red line indicates the downstream *Dommel*.

5 Discussion

5.1 Temporal evolution and spatial distribution drought indices

Data quality

Time series of precipitation, potential evaporation and groundwater are useful for temporal and spatial analysis of standardised indices. Spatial interpolation of runoff data is less useful due to limited spatial coverage (data availability), but these data are suitable for temporal analysis (Figure 4.3 and Figure 4.4). Soil moisture time series have an observation record of only 7 years which limits calculation of a variety of time scales. Due to the high resolution spatial distribution is possible (Figure 4.11), but only for short time scales.

Temporal evolution

Based on the dataset of precipitation, potential evaporation, soil moisture, discharge and groundwater levels we studied relations between the meteorological and hydrological drought. Speed of drought development and drought duration differ between the drought indices. Droughts become fewer and last longer when moving through the hydrological system which is in accordance with Van Loon et al. (2012). Time-series show how the effect of precipitation deficits propagate through soil moisture, runoff and groundwater variables (Figure 4.3 and Figure 4.4). The lag of the propagation of precipitation anomalies to the hydrological cycle can be found in Changnon (1987); Eltahir and Yeh (1999); Tallaksen and Van Lanen (2004). Not all meteorological droughts show up in the groundwater system because the soil moisture storage can be replenished before the drought is propagated to the groundwater.

Spatial distribution

The spatial distribution of meteorological drought is uniform distributed over Gelderland, whereas large regional differences exist in hydrological drought. Severe hydrological drought occurs in the groundwater observation wells in the low-lying areas of Gelderland with shallow groundwater tables because these areas react quick to changes in precipitation amounts. In the groundwater observation wells situated on the *Veluwe*, *Berg en Dal* and *Montferland* with deep groundwater tables we found wetter than normal conditions. The reason is that these areas have a slow response to changes in precipitation, even during severe precipitation deficits. When taking into account soil moisture, the spatial distribution is more related to meteorological drought because soil moisture quickly responds to changes in precipitation amounts.

5.2 Low flow indices

With a fixed threshold approach we are able to identify periods of low flow without seasonality. In The Netherlands during the summer period the discharge is generally lower compared to the winter period, to include this seasonality the variable threshold is used. The range of MAM1, MAM3, MAM7 and MAM30 was used because larger MAM values are less sensitive to measurement errors and additionally the day to day variations of the artificial component of the river flow are excluded (Smakhtin, 2001). Low flow indices are widely used to quantify some important low flow characteristics (Smakhtin, 2001). However, these indices does not provide a continuous index of drought that can provide insight into temporal structure in time series, such as autocorrelation (Bloomfield and Marchant, 2013).

5.3 Correlation between the indices

In our study we focussed on which accumulation period of SPI have the highest correlation with 1-month SGI. All the calculated correlations of the individual stations were significant proven by the Pearson test. The highest accumulation periods were found on the ridges of the province of Gelderland. The long time scales (over 6 months) are considered as hydrological drought indicators (McKee et al., 1993; Hayes et al., 1999). A case study in Hungary examined how strong the connection of SPI is with hydrological features, such as streamflow and groundwater levels (Bussay et al., 1998; Szalai and Szinell, 2000). Strong relationships to groundwater levels were found at time scales of 5--24 months, which is in line with our results. We assumed that all the aquifers were unconfined, but to interpret the SGI the hydrogeological structure (catchment characteristics) of a piezometer is important to take into account (Mendicino et al., 2008; Bloomfield and Marchant, 2013). Recharge processes and saturated flow processes have a high spatial variability.

5.4 Towards a new alternative of the KNMI index

The standardised indices have three main strengths, namely 1) simplicity, for example the SPI is solely based on precipitation; 2) the calculation for a variety of time scales, which allows to describe drought conditions for a range of meteorological, agricultural and hydrological applications; and 3) the estimated index values can be compared in space and time (Hayes et al., 1999; Lloyd-Hughes and Saunders, 2002; Mishra and Singh, 2010). But standardised indices also have limitations. The first limitation arises from the standardisation process. Extreme and severe droughts, when considered over a long time period, will occur with the same frequency at all location. The standardised index by itself cannot identify regions that may be more “drought prone” than others (Hayes et al., 1999; Lloyd-Hughes and Saunders, 2002). Furthermore problems can arise when fitting a probability distribution. Biased values can be reported when

long time scales (> 24 months) are calculated with short time series (Lloyd-Hughes and Saunders, 2002). These long time scales were not applied in our analysis.

A total combined drought index of the hydrological cycle can be used as alternative for the KNMI index; an example is the aggregate drought index (Keyantash and Dracup, 2004). To declare drought conditions only one indicator can be considered, but additional research is needed. To include the social-economic drought (Figure 2.1) different drought indices can be compared and based on the purpose of the specific stakeholder a choice can be made of the best applicable index. Furthermore identifying vulnerabilities can lead to adjustment in practices in water-dependent sectors (Sönmez et al., 2005).

We were interested to see if the KNMI index can capture the propagation of meteorological drought into hydrological drought by comparing this index with indices based on hydrological variables. In the province of Gelderland the results of SGI show that large temporal and spatial variations exist in the severity of hydrological drought. As a consequence of this variation the SPI, SPEI and KNMI index cannot simply represent hydrological drought conditions. Starting with relative dry conditions in the growing season can have large consequences for the agriculture sector (and other related sectors), therefore standardised indices are an appropriate tool to monitor different types of drought.

6 Conclusions and recommendations

6.1 Conclusions

In this study we studied the difference between the operational KNMI drought index and some selected drought indices for the province of Gelderland, The Netherlands. The KNMI index calculates the cumulative rainfall deficit for the period April till September, the other indices take into account the whole year. The selected drought indices based on different variables show the same major droughts. Drought indices based on precipitation and potential evaporation are more variable in time while drought indices based on discharge and groundwater have a smoothed signal. Spatial distribution of a meteorological drought shows a uniform pattern over Gelderland, whereas large regionally differences exist in the severity of a hydrological drought. Areas with deep groundwater tables experience still wet conditions during selected drought events, caused by the slow response to changes in precipitation. Furthermore the possibility of a new drought index for The Netherlands was investigated. Data availability and quality is good for time series of precipitation, potential evaporation and groundwater. The length of available data of soil moisture is too short to calculate a variety of time scales. Runoff data are less applicable due to the limited spatial coverage. Meteorological drought indices (like the index used by the KNMI) cannot simply be used to represent hydrological drought conditions due to differences in temporal and spatial variation.

6.2 Recommendations

This study leads to the following recommendations:

- For this thesis the gamma and genlog probability distributions were applied. More probability distributions exist and a comparison can be made which give the best fit for the different drought indices.
- Complete and reliable time series are needed to get an improved quality of the standardised values. Limiting factor is the availability of the time series from different sources.
- This study can be elaborated to more provinces in The Netherlands. The SPI, SPEI and SGI are the most useful indices due to the good data availability. Differences between the indices and the KNMI maps of the 12 provinces can be investigated.
- Waterboards can built up a national network for measuring and store runoff data. The waterboards should collaborate together in order to get a central data base which improves the data quality.
- A follow-up study can take into account the geology of the province to know if a well is in an unconfined or confined aquifer. The statistical analyses can then be more specifically elaborated per location.

- The coupling between the drought indices and specific stakeholder can be investigated. Questions are: “Where is the biggest social-economic impact of a drought? Which drought index will give the best prediction?”

Bibliography

AHN (2014). Digital elevation data of the netherlands. `www.ahn.nl`.

Alley, W. (1984). The palmer drought severity index: limitations and assumptions. *Journal of climate and applied meteorology*, 23(7):1100--1109.

Beyene, B., Van Loon, A., Van Lanen, H., and Torfs, P. (2014). Investigation of variable threshold level approaches for hydrological drought identification to be submitted. *Hydrology and Earth System Sciences Discussion*.

Bhuiyan, C. (2004). Various drought indices for monitoring drought condition in aravalli terrain of india. In *XXth ISPRS Congress*, pages 12--23.

Bhuiyan, C., Singh, R., and Kogan, F. (2006). Monitoring drought dynamics in the aravalli region (india) using different indices based on ground and remote sensing data. *International Journal of Applied Earth Observation and Geoinformation*, 8(4):289--302.

Bloomfield, J. and Marchant, B. (2013). Analysis of groundwater drought building on the standardised precipitation index approach. *Hydrology & Earth System Sciences*, 17(12):4769--4787.

Buishand, T. and Velds, C. (1980). *Klimaat van Nederland 1: Neerslag en verdamping*. KNMI.

Bussay, A., Szinell, C., Hayes, M., and Svoboda, M. (1998). Monitoring drought in hungary using the standardized precipitation index. In *Annales Geophysicae, Supplement*, volume 11.

Changnon, S. (1987). *Detecting drought conditions in Illinois*. Illinois State Water Survey.

Dinoloket (2014). Geohydrological data bank. `www.dinoloket.nl`.

Eltahir, E. and Yeh, P. (1999). On the asymmetric response of aquifer water level to floods and droughts in illinois. *Water Resources Research*, 35(4):1199--1217.

Fink, A., Brücher, T., Krüger, A., Leckebusch, G., Pinto, J., and Ulbrich, U. (2004). The 2003 european summer heatwaves and drought--synoptic diagnosis and impacts. *Weather*, 59(8):209--216.

Gibbs, W. and Maher, J. (1967). Rainfall deciles as drought indicators. *Australian bureau of Meteorology*.

Goovaerts, P. (1997). *Geostatistics for natural resources evaluation*. Oxford university press.

Gudmundsson, L. and Stagge, J. (2014). *SCI: Standardized Climate Indices such as SPI, SRI or SPEI*. R package version 1.0-0.

Guttman, N. (1999). Accepting the standardized precipitation index: A calculation algorithm1. *JAWRA Journal of the American Water Resources Association*, 35(2):311--322.

Hayes, M., Svoboda, M., Wilhite, D., and Vanyarkho, O. (1999). Monitoring of the 1996 drought using the standardized precipitation index. *Bulletin of the American Meteorological Society*, 89:429--438.

Heim, R. (2002). A review of twentieth-century drought indices used in the united states. *Bulletin of the American Meteorological Society*, 83(8):1149--1165.

Hiemstra, P. and Sluiter, R. (2011). *Interpolation of Makkink evaporation in the Netherlands*. KNMI.

Hindley, D. (1973). The definition of dry weather flow in river flow measurement. *J. Inst. Water Engng*, 27:438--440.

Hisdal, H., Tallaksen, L., Peters, E., Stahl, K., and Zaidman, M. (2000). Drought event definition. *ARIDE Technical Rep*, 6.

Hooghart, J. and Lablans, W. (1988). Van penman naar makkink: een nieuwe berekeningswijze voor de klimatologische verdampingsgetallen. Technical report, KNMI.

Hunt, E., Hubbard, K., Wilhite, D., Arkebauer, T., and Dutcher, A. (2009). The development and evaluation of a soil moisture index. *International Journal of Climatology*, 29(5):747--759.

Huza, J., Teuling, A., Braud, I., Grazioli, J., Melsen, L., Nord, G., Raupach, T., and Uijlenhoet, R. (2014). Precipitation, soil moisture and runoff variability in a small river catchment (ardèche, france) during hymex special observation period 1. *Journal of Hydrology*, 516:330--342.

Institute of Hydrology (1980). Low flows studies report (1-4). Technical report, Wallingford, UK.

IPCC (2014). Climate change 2014: Impacts, adaptation, and vulnerability. part a: Global and sectoral aspects. contribution of working group ii to the fifth assessment report of the intergovernmental panel on climate change. [Field, C.B., V.R. Barros, D.J. Dokken, K.J. Mach, M.D. Mastrandrea, T.E. Bilir, M. Chatterjee, K.L. Ebi, Y.O. Estrada, R.C. Genova, B. Girma, E.S. Kissel, A.N. Levy, S. MacCracken, P.R. Mastrandrea, and L.L. White (eds.)]. Cambridge University Press, Cambridge, United Kingdom and New York, NY, USA.

Kendall, M. and Alan, S. (1961). *The advanced theory of statistics. Vols. II and III.* Hafner.

Keyantash, J. and Dracup, J. (2002). The quantification of drought: An evaluation of drought indices. *Bulletin of the American Meteorological Society*, 83(8):1167--1180.

Keyantash, J. and Dracup, J. (2004). An aggregate drought index: Assessing drought severity based on fluctuations in the hydrologic cycle and surface water storage. *Water Resources Research*, 40(9).

KNMI (2014). Climatological data bank. `www.knmi.nl`.

Lloyd-Hughes, B. and Saunders, M. (2002). A drought climatology for europe. *International Journal of Climatology*, 22(13):1571--1592.

Longley, P. (2005). *Geographic information systems and science*. John Wiley & Sons.

Makkink, G. (1957). Testing the penman formula by means of lysimeters. *J. Inst. Water Eng*, 11(3):277--288.

Marsh, T. (2004). The uk drought of 2003: a hydrological review. *Weather*, 59(8):224--230.

McEvoy, D., Huntington, J., Abatzoglou, J., and Edwards, L. (2012). An evaluation of multiscalar drought indices in nevada and eastern california. *Earth Interactions*, 16(18):1--8.

McKee, T., Doesken, N., and Kleist, J. (1993). 8th conference on applied climatology. In *The relationship of drought frequency and duration to time scales*, pages 179--184.

Mendicino, G., Senatore, A., and Versace, P. (2008). A groundwater resource index (gri) for drought monitoring and forecasting in a mediterranean climate. *Journal of Hydrology*, 357(3):282--302.

Mishra, A. and Singh, V. (2010). A review of drought concepts. *Journal of Hydrology*, 391(1):202--216.

Morid, S., Smakhtin, V., and Moghaddasi, M. (2006). Comparison of seven meteorological indices for drought monitoring in iran. *International journal of climatology*, 26(7):971--985.

Narasimhan, B. and Srinivasan, R. (2005). Development and evaluation of soil moisture deficit index (smdi) and evapotranspiration deficit index (etdi) for agricultural drought monitoring. *Agricultural and Forest Meteorology*, 133(1):69--88.

Okabe, A., Boots, B., Sugihara, K., and Chiu, S. (2009). *Spatial tessellations: concepts and applications of Voronoi diagrams*. John Wiley & Sons.

Orlowsky, B. and Seneviratne, S. (2013). Elusive drought: uncertainty in observed trends and short-and long-term cmip5 projections. *Hydrology and Earth System Sciences*, 17(5):1765--1781.

Owe, M., de Jeu, R., and Holmes, T. (2008). Multi-sensor historical climatology of satellite-derived global land surface moisture. *Journal of Geophysical Research*, 113.

Palmer, W. (1968). Keeping track of crop moisture conditions, nationwide: The new crop moisture index. *Weatherwise*, 21:156--161.

Palmer, W. C. (1965). *Meteorological drought*. US Department of Commerce, Weather Bureau Washington, USA.

Peters, E., Bier, G., Van Lanen, H., and Torfs, P. (2006). Propagation and spatial distribution of drought in a groundwater catchment. *Journal of hydrology*, 321(1):257--275.

Peters, E., Torfs, P., Van Lanen, H., and Bier, G. (2003). Propagation of drought through groundwater - a new approach using linear reservoir theory. *Hydrological processes*, 17(15):3023--3040.

Pirt, J., Simpson, M., and Authority, S. T. W. (1983). *The Estimation of river flows*. Severn Trent Water Authority.

Rebetez, M., Mayer, H., Dupont, O., Schindler, D., Gartner, K., Kropp, J., and Menzel, A. (2006). Heat and drought 2003 in europe: a climate synthesis. *Annals of Forest Science*, 63(6):569--577.

Searcy, J. (1959). *Flow-duration curves*. US Government Printing Office.

Shafer, B. and Dezman, L. (1982). Development of a surface water supply index (swsi) to assess the severity of drought conditions in snowpack runoff areas. In *Proceedings of the Western Snow Conference*, volume 50, pages 164--175.

Shepard, D. (1968). A two-dimensional interpolation function for irregularly-spaced data. In *Proceedings of the 1968 23rd ACM national conference*, pages 517--524. ACM.

Shukla, S. and Wood, A. (2008). Use of a standardized runoff index for the characterizing hydrologic drought. *Geophysical research letters*, 35:1--7.

Smakhtin, V. (2001). Low flow hydrology: a review. *Journal of hydrology*, 240(3):147--186.

Sönmez, F., Koemuescue, A. U., Erkan, A., and Turgu, E. (2005). An analysis of spatial and temporal dimension of drought vulnerability in turkey using the standardized precipitation index. *Natural Hazards*, 35(2):243--264.

Stagge, J., Tallaksen, L., Gudmundsson, L., Van Loon, A., and Stahl, K. (2013). Pan-european comparison of candidate distributions for climatological drought indices, spi and spei. In *EGU General Assembly Conference Abstracts*, volume 15, page 9329.

Szalai, S. and Szinell, C. (2000). Comparison of two drought indices for drought monitoring in hungary—a case study. In *Drought and drought mitigation in Europe*, pages 161--166. Springer.

Tallaksen, L. and Van Lanen, H. (2004). *Hydrological Drought: Processes and Estimnation Methods for Streamflow and Groundwater*, volume 48. Elsevier.

Teuling, A., Van Loon, A., Seneviratne, S., Lehner, I., Aubinet, M., Heinesch, B., Bernhofer, C., Grünwald, T., Prasse, H., and Spank, U. (2013). Evapotranspiration amplifies european summer drought. *Geophysical Research Letters*, 40(10):2071--2075.

Van Loon, A., Van Huijgevoort, M., and Van Lanen, H. (2012). Evaluation of drought propagation in an ensemble mean of large-scale hydrological models. *Hydrology and Earth System Sciences Discussions*, 9(7):8375--8424.

Van Loon, A. and Van Lanen, H. (2012). A process- based typology of hydrological dorught. *Hydrology and Earth System Sciences*, 16:1915--1942.

Van Rooy, M. (1965). A rainfall anomaly index independent of time and space. *Notos*, 14:43--48.

Vicente-Serrano, S., Begueria, S., and Lopez-Moreno, J. (2009). A muliscalar drought index sensitive to global warming: the standardized precipitation evaporation index. *Journal of Climate*, 23:1696--1718.

Wanders, N., Karssenberg, D., Bierkens, M., Parinussa, R., de Jeu, R., van Dam, J., and de Jong, S. (2012). Observation uncertainty of satellite soil moisture products determined with physically-based modeling. *Remote Sensing of Environment*, 127:341--356.

Wanders, N., Van Lanen, H., and Van Loon, A. (2010). Indicators for drought characterization on a global scale. Technical report, Watch. Water and global change.

Wilhite, D. (2006). Drought monitoring and early warning: Concepts, progress and future challenges. *World Meteorological Organization*.

Yevjevich, V. (1967). *An objective approach to definitions and investigations of continental hydrologic droughts*. Colorado State University Fort Collins.

A Manual and automatic rain gauge network The Netherlands

Figure A.1: Manual rain gauge network in The Netherlands (KNMI, 2014).

Figure A.2: Automatic rain gauge network in The Netherlands (KNMI, 2014).

B Catchment description

Brabantse Delta

The source of the *Donge* is near the village of Dongen and flows north where it merges with the *Amer* and *Bergse Maas*.

De Dommel

The *Beerze* is a brook in the province of Noord-Brabant. The *Grote Beerze* and the *Kleine Beerze* are part of the upstream area. Just before Boxtel a side-branch, the *Kleine Aa*, flows into the *Essche stroom*. The main branch joins the river the *Dommel*.

The *Dommel* flows partly in Belgium (35 km), but for the main part in The Netherlands (85 km). The *Dommel* starts at the *Kempens* plateau and the total slope of 75 m. During wet periods the discharge can increase enormously and during dry periods the discharge is only a few meters per second.

The *Essche stroom* has only a length of 7 km. Like many other brooks also the *Essche stroom* was channelled. The waterboard wants to improve the water quality and nature development along this brook.

The *Nieuwe Leij* is a brook in the province of Noord-Brabant. It has two different sources, both very close at the Belgium boder near the village Poppel.

The *Tongelreep* is a sidebranch of the river the *Dommel*. The source of this river is in Belgium. After passing several small villages it crosses the Dutch border and flows in the direction of Eindhoven. It is known of is water clarity.

Hunze en Aa

The *Hunze* is a river located in the border area between the provinces of Drenthe and Groningen. The waterboard Hunze and Aa started a project to restore the old meanders and a natural landscape.

Rijn en IJssel

The *Berkel* starts in Germany, flows through the Achterhoek to join the *IJssel* at Zutphen after about 110 kilometres. The waterboard Rijn en IJssel is responsible for the management of the Dutch part. Different side-branches join the *Berkel*.

The *Bovenslinge* starts in Germany and joins the *Oude IJssel* in Gaanderen. Part of the river is changed to its former state.

The *Hupsel* is a small brook in eastern part of Gelderland. This small catchment is measured by the chairgroup Hydrology and Quantitative Water Management of the WUR.

The *Oude IJssel* starts in Germany and flows southwest until Wesel and then turns northwest. After Isselburg it crosses the border with The Netherlands and joins the *IJssel* in Doesburg. The river is approximately 80 km long.

The *Schipbeek* is a branch of the river the *IJssel* and starts in Germany. It flows through a large part of the Achterhoek and the south of Twente. During high discharge periods the water can flow into the *Twentekanaal* and during low discharge visa versa.

Roer en Overmaas

The *Geleenebeek* is for a large part situated in the national landscape of Zuid-Limburg. The source is in the small village Benzenrade. It flows generally northwest, through the centre of Sittard until it flows into the *Meuse*. It is the largest catchment within the area of the waterboard.

The *Geul* starts in Belgium and flows northward to The Netherlands. It is a tributary of the river the *Meuse*. The river has a total length of 58 km and a slope of 250 m. Former canalisation is largely removed, which means that the river meanders again. A tributary to this river is the *Gulp*.

The *Roer* is also a tributary of the *Meuse*. The total length is 165 km, only 21.5 km is on Dutch territory. The source is in Belgium, but a significant part of th river flows in Germany. A lot of tributaries join the *Roer*, wherefore the discharge increases. In Germany the river is dammed. The water quality increased a lot during the last decade.

Velt en Vecht

The *Vecht* is a precipitation fed river in Germany and The Netherlands. It has a total length of 167 km, where 60 km is situated within the Dutch border. The *Vecht* originates in the *Baumberge* hills of Germany, flows northward and finally westward into the Dutch province of Overijssel. The water of the Regge stream merge into the *Vecht* and close to the city Zwolle it joins the river the *Zwarte Water*.

Rijkswaterstaat

Rijkswaterstaat is responsible for the large rivers in The Netherlands, such as the *Rhine*, the *Waal* and the *Meuse*. The catchments of these rivers are situated outside The Netherlands. The reason to include measurement points of these rivers is to compare drought periods in The Netherlands with France and Switzerland. The weather systems in these countries are most of the time responsible for wet and / or dry periods. Also situations the other way around can happen, such as drought in the Alps and very wet

conditions in The Netherlands. The consequence is a low discharge in the large rivers compared with a increasing discharge in the small brooks / streams.

C Groundwater wells

Table C.1: Overview of the selected groundwater wells

Well	X-coordinate [m]	Y-coordinate [m]	Years with observed groundwater
B26H0044	176720	484170	02-12-1948 / 15-04-2013
B26H0145	170100	480580	01-12-1967 / 30-09-2013
B27A0259	185980	494820	14-08-1968 / 04-04-2013
B27B0155	190800	488240	25-03-1969 / 04-04-2013
B27C0049	183760	476425	16-07-1971 / 23-07-2013
B27D0053	197100	477530	29-07-1974 / 04-06-2013
B27E0138	200220	495500	10-04-1973 / 11-06-2013
B32E0091	166610	469210	15-01-1990 / 08-04-2013
B32F0065	170460	466770	26-06-1967 / 08-04-2013
B32G0139	160030	452679	16-11-1972 / 04-11-2010
B32H0094	178260	451670	31-10-1961 / 17-12-2012
B32H0108	173425	460730	11-12-1963 / 05-09-2013
B32H0393	172230	450300	14-08-1974 / 20-12-2012
B33A0067	181030	463970	20-09-1927 / 02-04-2013
B33B0325	190890	468670	28-11-1988 / 23-07-2013
B33C0135	188950	460520	23-11-1961 / 10-03-2013
B33D0271	197050	453260	06-05-1964 / 26-04-2012
B33E0377	203000	462880	28-12-1971 / 03-06-2013
B33F0181	214260	470790	14-01-1981 / 25-06-2013
B33G0351	209870	456600	28-02-1966 / 20-09-2013
B34A0108	229920	465930	29-10-1990 / 09-07-2013
B34C0040	227180	452900	20-10-1966 / 29-07-2013
B34D0335	237020	451160	14-02-1972 / 16-09-2013
B34E0300	243340	463590	14-10-1965 / 14-11-2013
B34G0264	245570	458910	07-05-1963 / 10-09-2013
B39C0104	142580	429140	14-10-1968 / 15-07-2013
B39C0150	141130	436120	15-01-1990 / 15-07-2013
B39D0224	151600	427720	15-01-1990 / 15-07-2013
B39D0299	154150	434970	14-04-1953 / 13-04-2007
B39E0093	163000	438030	14-05-1968 / 28-05-2013
B39F0300	173030	438220	10-07-1975 / 28-5-2013
B39G0275	165050	430140	14-07-1988 / 11-07-2012
B39H0014	175280	427480	14-06-1950 / 14-03-2014
B40A0214	183508	439739	14-02-1962 / 27-05-2013
B40A0550	188249	448870	15-06-1990 / 31-05-2013
B40B0447	196350	442310	14-01-1953 / 02-05-2012
B40C0414	184710	435500	27-05-1977 / 28-05-2013
B40D0151	196410	427900	28-09-1988 / 11-11-2012
B40E0253	200490	449340	28-3-1989 / 01-07-2013
B40H0047	214190	435940	02-03-1970 / 2303-2009
B41A0171	221210	441470	14-02-1972 / 14-09-2011
B41B0189	234910	437980	13-10-1952 / 08-08-2013
B41D0013	231770	433020	16-12-1969 / 01-03-2011
B41E0405	249100	439750	29-08-1975 / 20-08-2013
B44F0097	139490	422920	21-07-1971 / 17-02-2013
B45A0006	143730	421640	28-11-1962 / 07-10-2013
B45B0308	154387	420384	28-02-1983 / 09-10-2013
B46A0140	189595	422847	28-01-1975 / 29-08-2013
B46A0717	182110	422650	28-12-1990 / 29-08-2013

D QQ-plots of soil moisture time series

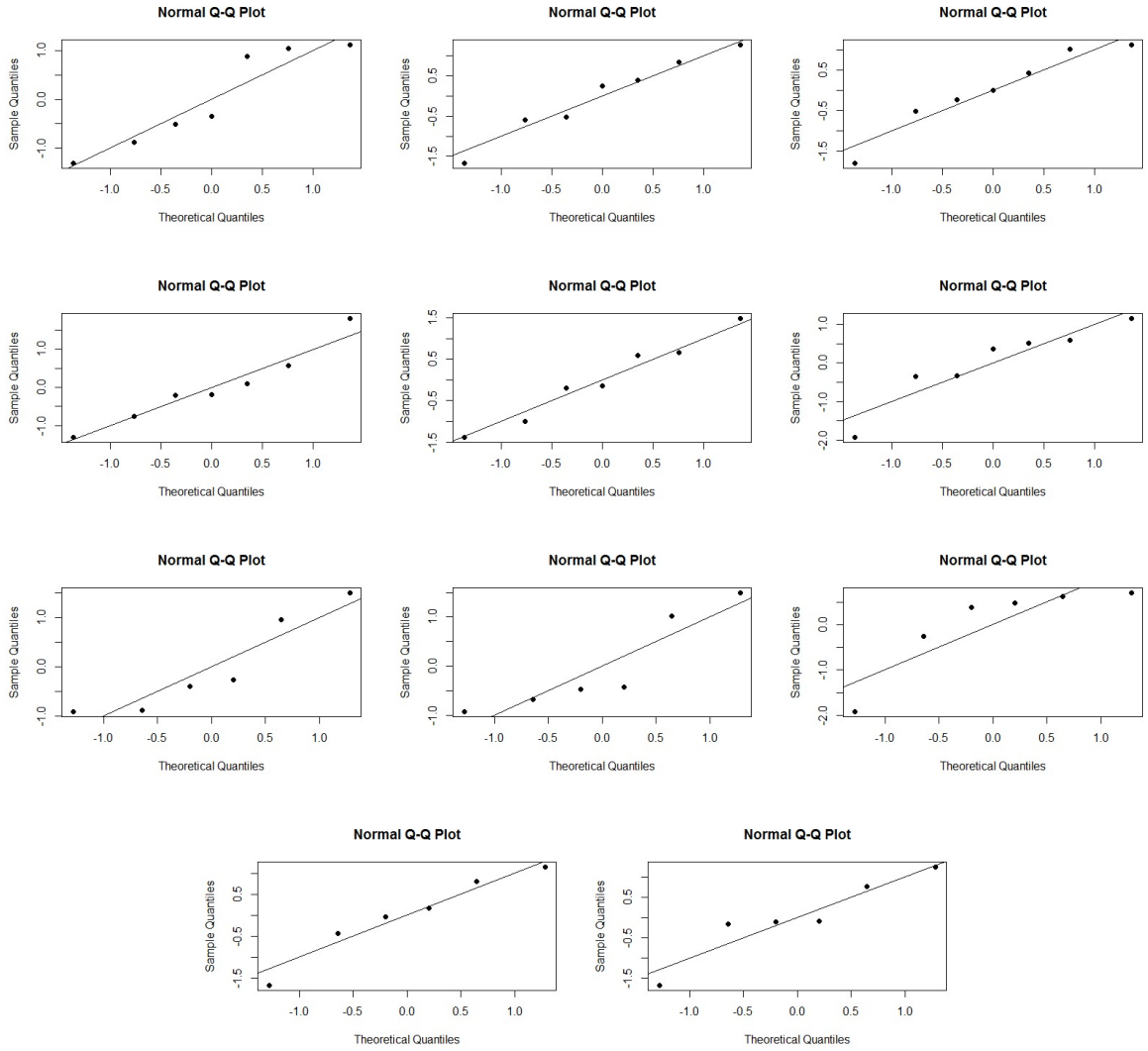

Figure D.1: QQ-plots of the all different months from 2007 till 2013.

E Comparison interpolated maps

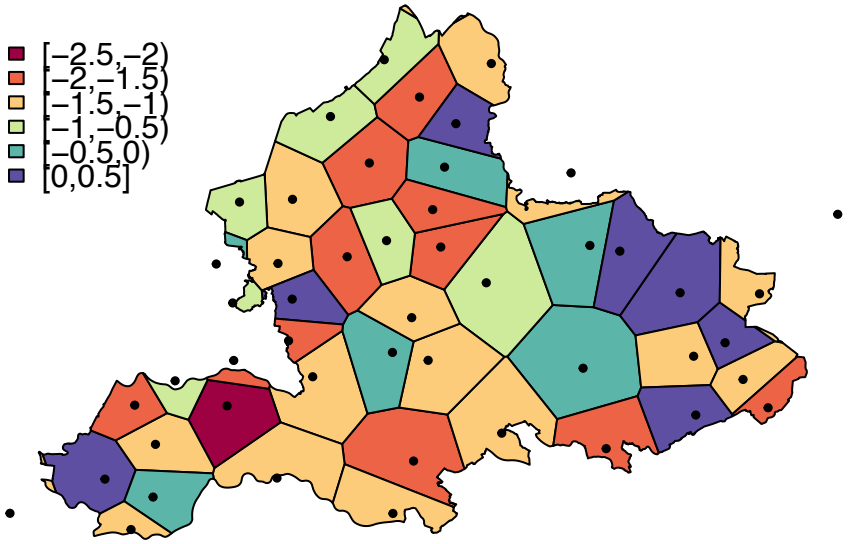

Figure E.1: An example of the applied interpolation technique Thiessen Polygons.

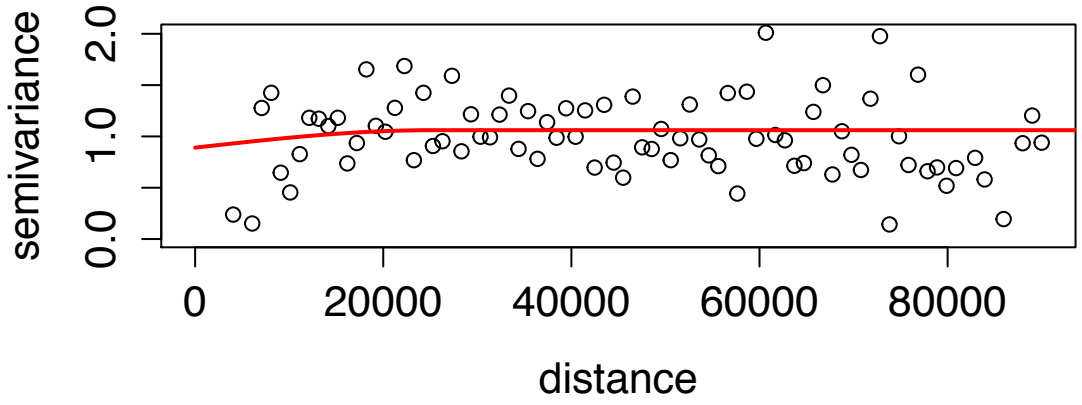

Figure E.2: Fit of the semivariogram model of groundwater time series.

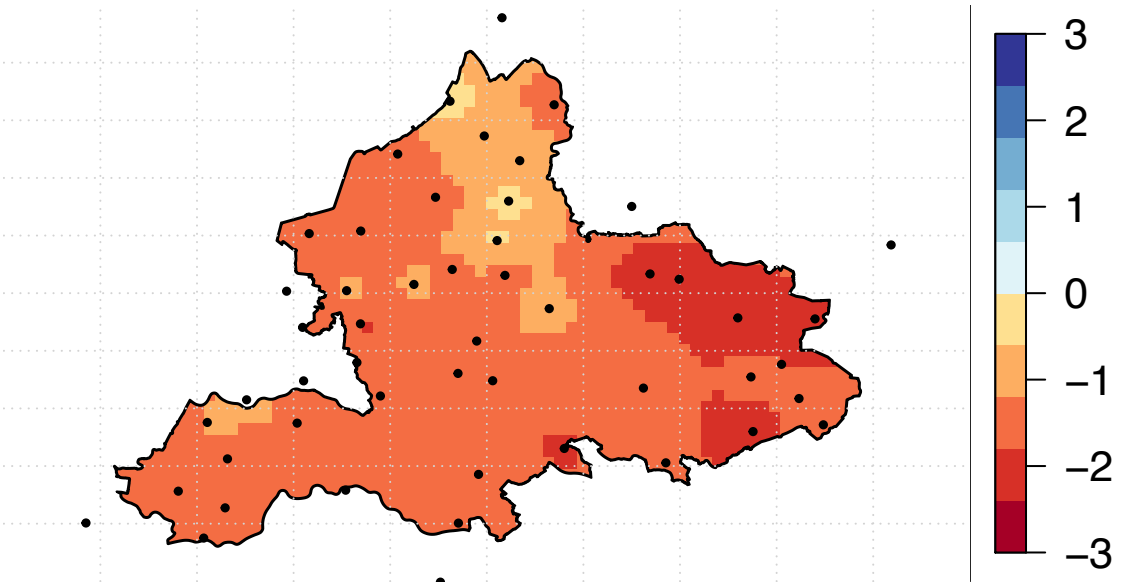

Figure E.3: The 6-month SPEI of September 2009 with the applied interpolation technique IDW.

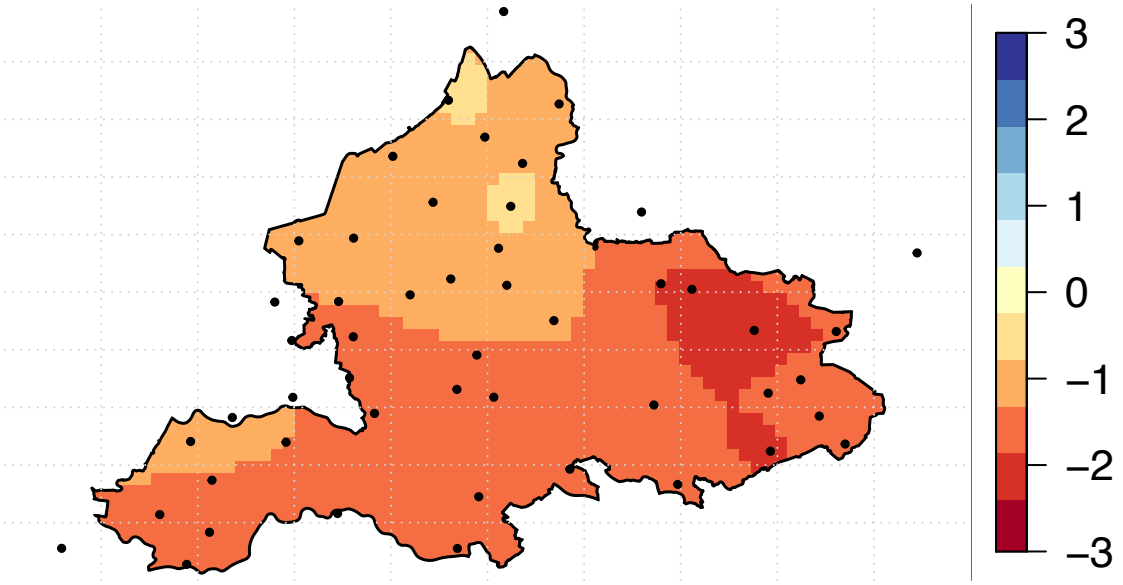

Figure E.4: The 6-month SPEI of September 2009 with the applied interpolation technique ordinairy kriging.

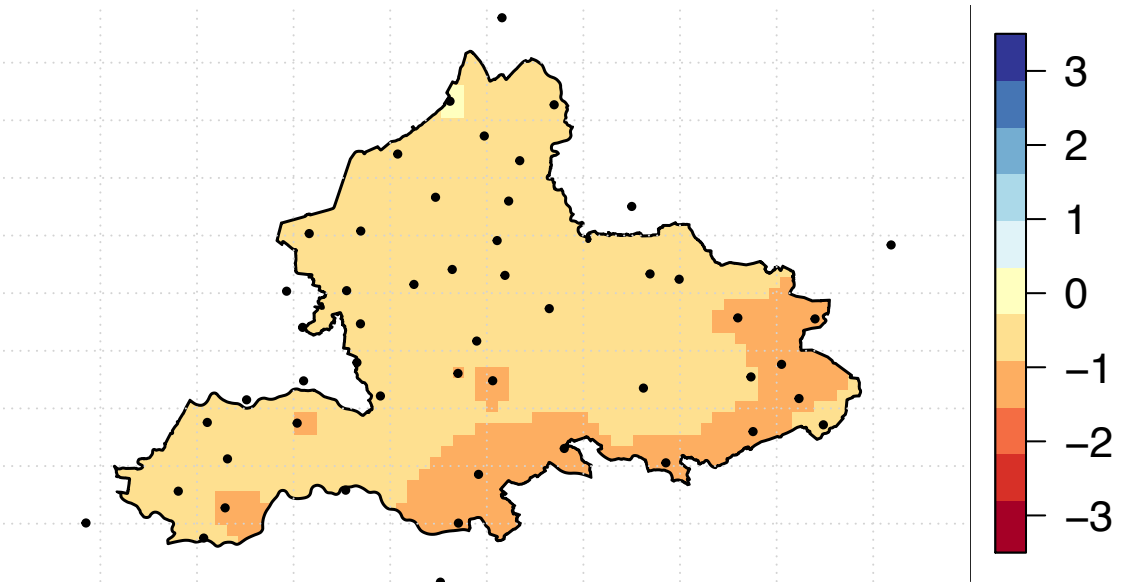

Figure E.5: The 3-month SPEI of January 1998 with the applied interpolation technique IDW.

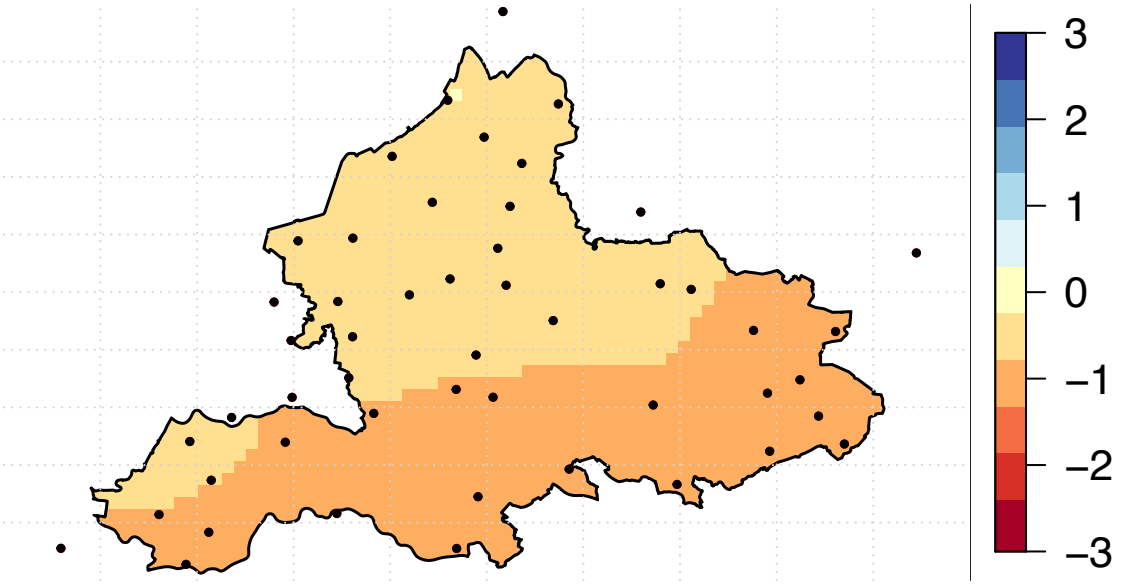

Figure E.6: The 3-month SPEI of January 1998 with the applied interpolation technique ordinairy kriging.

F 1-month SPI, SPEI, SRI and SGI

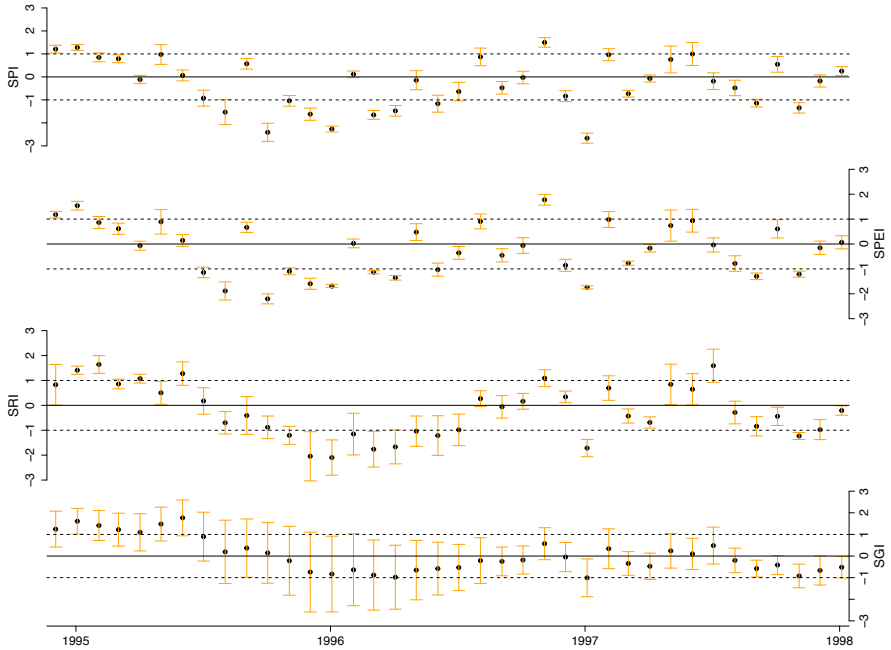

Figure F.1: The 1-month SPI, SPEI, SRI and SGI for 1995-1997 with error bars. The error bars represent the spatial standard deviation of every month.

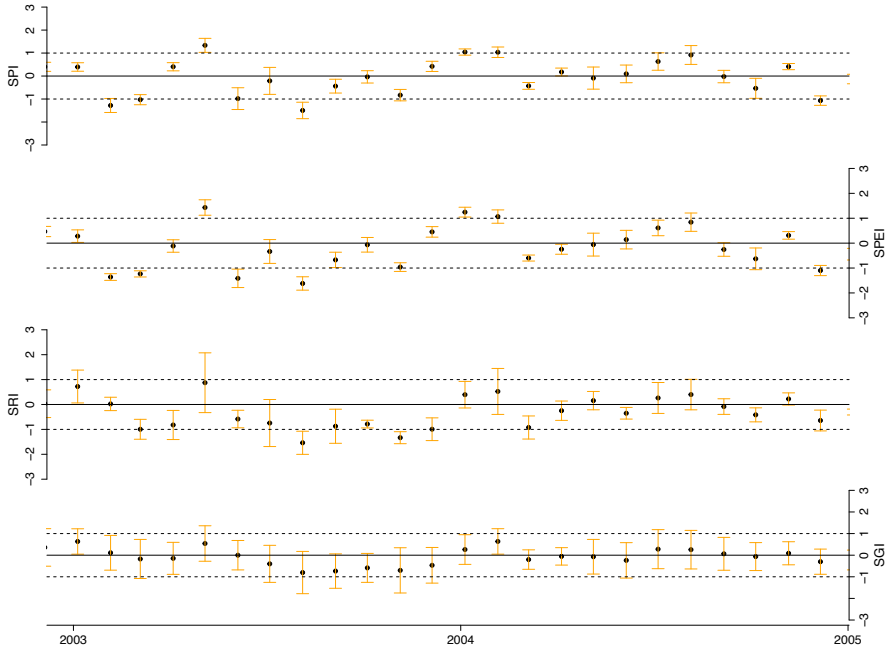

Figure F.2: The 1-month SPI, SPEI, SRI and SGI for 2003-2004 with error bars. The error bars represent the spatial standard deviation of every month.

G 6-month SPI, SPEI, SRI and SGI

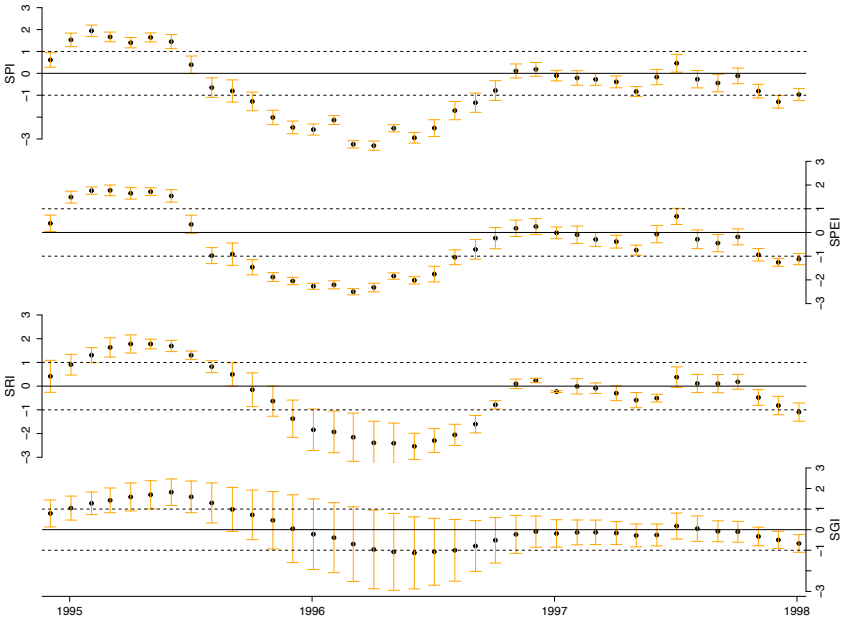

Figure G.1: The 6-month SPI, SPEI, SRI and SGI for 1995-1997 with error bars. The error bars represent the spatial standard deviation of every month.

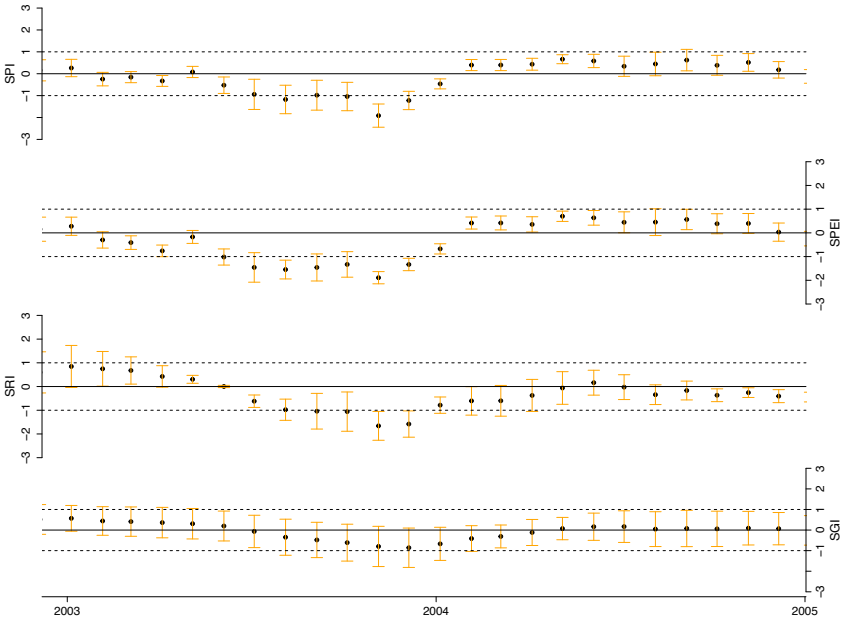

Figure G.2: The 6-month SPI, SPEI, SRI and SGI for 2003-2004 with error bars. The error bars represent the spatial standard deviation of every month.

H Statistical results

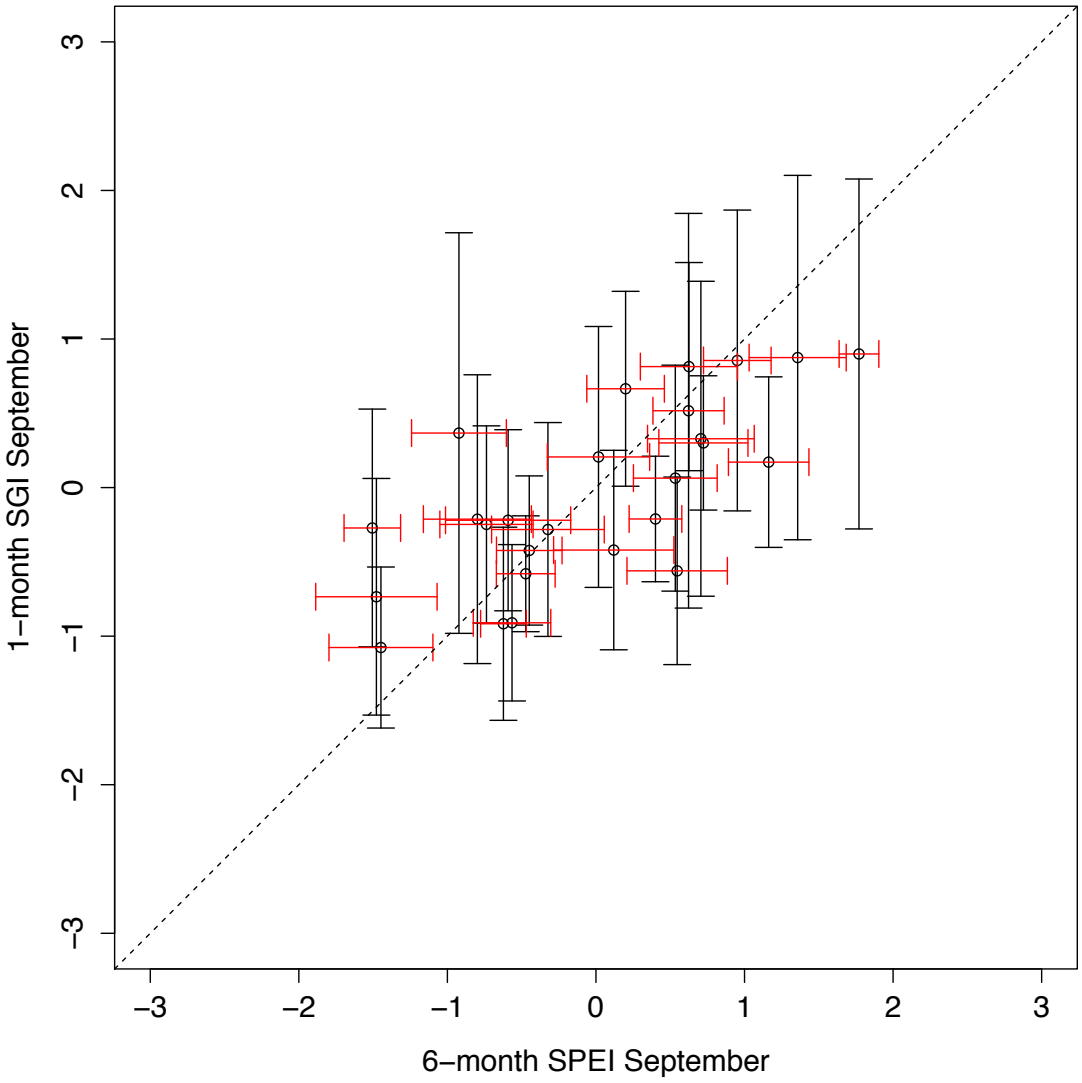

Figure H.1: Mean and standard deviation of 6-month SPEI of the September months (1988-2013) versus 1-month SGI of the September months (1988-2013).

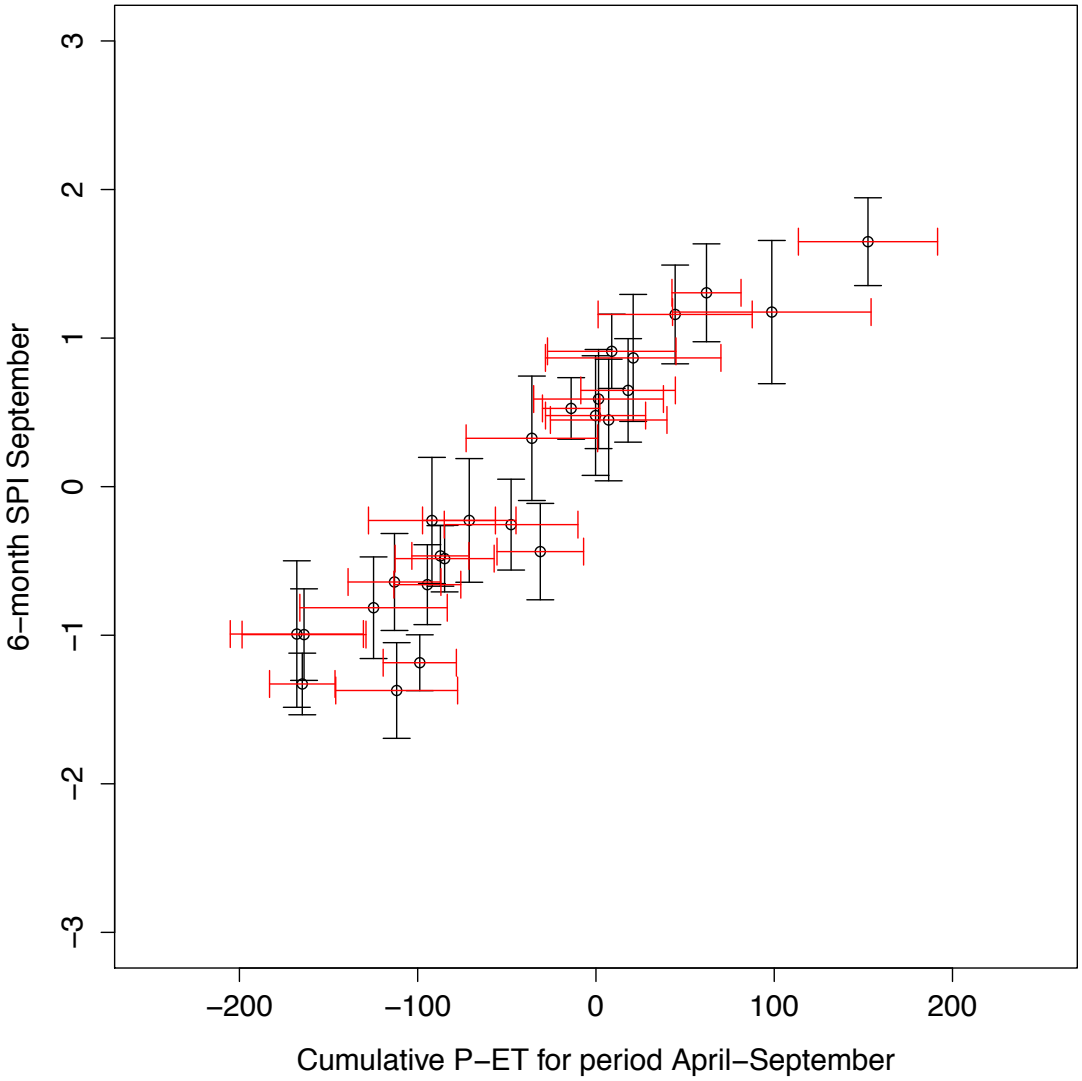

Figure H.2: Mean and standard deviation of cumulative precipitation minus evaporation of the period April till September (1988-2013) versus 6-month SPI of the September months (1988-2013).

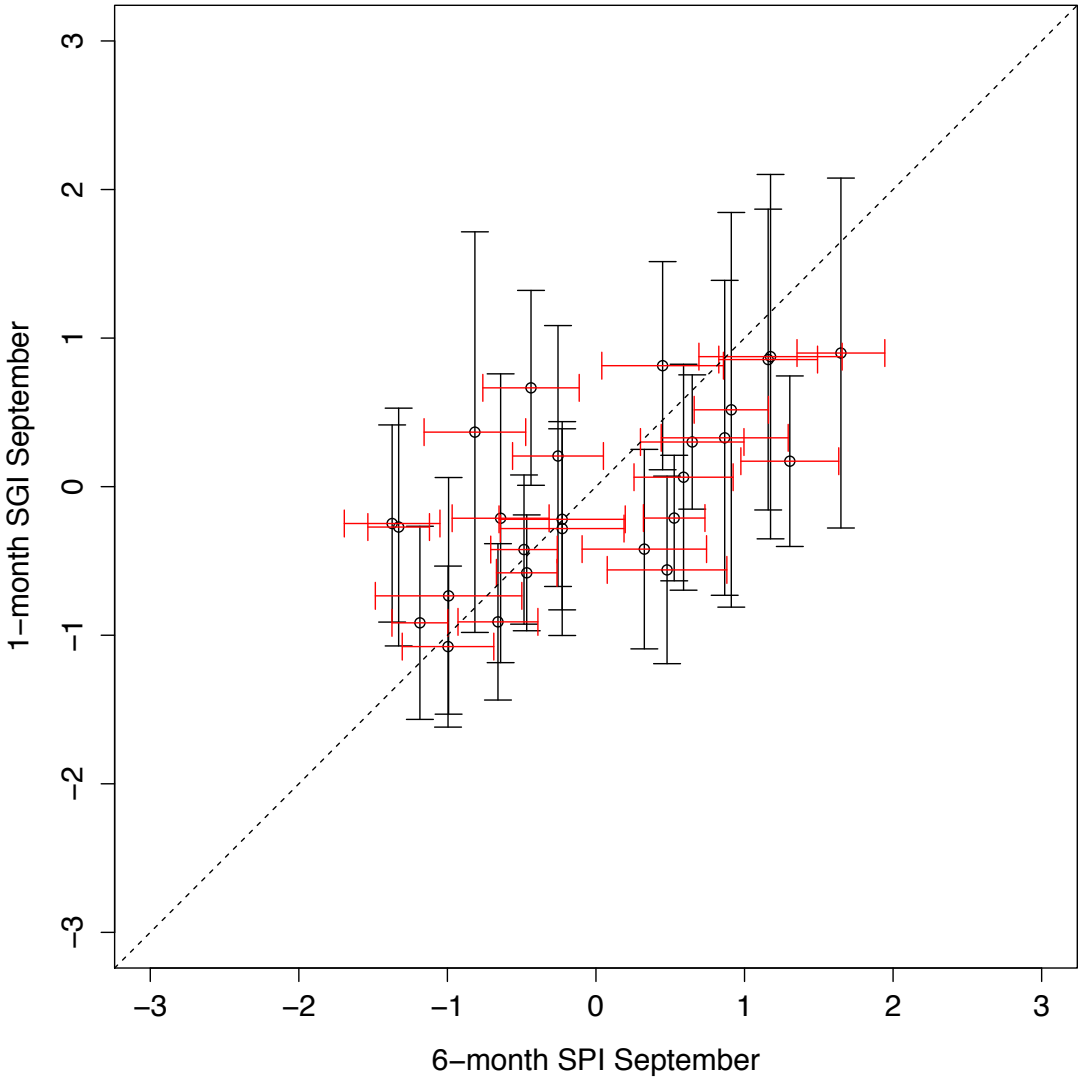

Figure H.3: Mean and standard deviation of 6-month SPI of the September months (1988-2013) versus 1-month SGI of the September months (1988-2013).

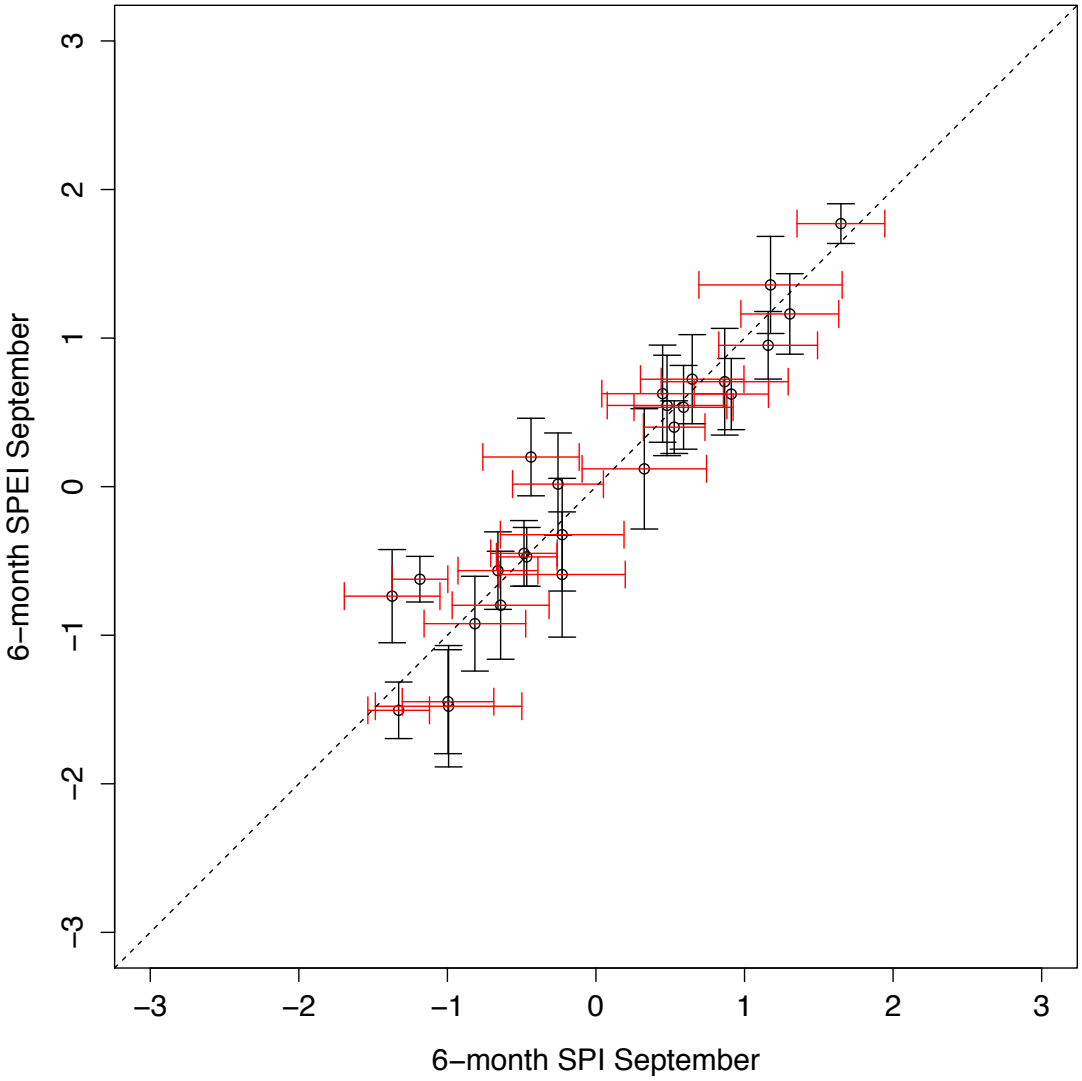

Figure H.4: Mean and standard deviation of 6-month SPI of the September months (1988-2013) versus 6-month SPEI of the September months (1988-2013).

I Overview low flow indices

Table I.1: Overview of low flow indices for the selected rivers

	Meanflow $[\frac{m^3}{s}]$	MAM1 $[\frac{m^3}{s}]$	MAM3 $[\frac{m^3}{s}]$	MAM7 $[\frac{m^3}{s}]$	MAM30 $[\frac{m^3}{s}]$	Q70 $[\frac{m^3}{s}]$	Q90 $[\frac{m^3}{s}]$	Q95 $[\frac{m^3}{s}]$	BFI
Beerze	0.68	1.36×10^{-2}	2.19×10^{-2}	3.11×10^{-2}	8.93×10^{-2}	0.15	5×10^{-2}	1×10^{-2}	0.528
Berkel	4.41	0.875	0.937	1.03	1.32	1.79	1.17	0.984	0.612
Bovenslinge	0.887	0.107	0.113	0.124	0.23	0.216	1×10^{-1}	6.7×10^{-2}	0.497
Dommel	13.9	3.47	3.82	4.18	5.3	7.42	5.09	4.24	0.658
Donge	0.638	4.37×10^{-2}	6.84×10^{-2}	9.23×10^{-2}	0.164	0.25	7.1×10^{-2}	4×10^{-2}	0.587
Essche stroom	3.11	0.529	0.607	0.659	0.874	1.39	0.83	0.666	0.636
Geelebeek	0.516	4.74×10^{-2}	4.94×10^{-2}	5.8×10^{-2}	9.39×10^{-2}	0.179	5.5×10^{-2}	1.8×10^{-2}	0.655
Geleenbeek	2.75	1.47	1.52	1.59	1.84	1.9	1.52	1.38	0.707
Geul	3.27	1.5	1.56	1.61	1.81	2.04	1.6	1.46	0.726
Groenlosche Slinge	1.45	0.158	0.181	0.22	0.443	0.571	0.219	0.123	0.449
Hunze	0.944	4.15×10^{-2}	6.97×10^{-2}	0.11	0.213	0.42	0.21	0.12	0.527
Hupsel	6.3×10^{-2}	2×10^{-3}	2.2×10^{-3}	2.5×10^{-3}	4.1×10^{-3}	7.9×10^{-3}	3×10^{-3}	2×10^{-3}	0.397
Meuse	230	9.03	11.2	15.3	23.5	58	16	10.1	0.541
Nieuwe Leij	0.907	0.102	0.111	0.124	0.194	0.242	9.1×10^{-2}	6.1×10^{-2}	0.512
Oude IJssel	8.99	0.725	0.836	0.94	1.76	2.89	1.12	0.648	0.624
Regge	9.43	1.43	1.73	2.05	2.92	4.67	2.7	2.17	0.625
Reusel	1.45	0.123	0.149	0.17	0.29	0.51	0.23	0.163	0.559
Rhine	2215	1075	1084	1106	1242	1548	1221	1102	0.834
Roer	21.3	10.5	10.7	11.1	12.3	14.3	11.6	10.5	0.772
Schipbeek	1.37	0.135	0.165	0.18	0.235	0.333	0.183	0.149	0.44
Springendalsebeek	4.71×10^{-2}	1.61×10^{-2}	1.76×10^{-2}	2×10^{-2}	2.53×10^{-2}	3.2×10^{-2}	2.3×10^{-2}	1.9×10^{-2}	0.755
Tongelreep	0.844	0.313	0.333	0.358	0.478	6×10^{-1}	4×10^{-1}	3×10^{-1}	0.756
Vecht	17.9	3.05	3.46	3.71	5.24	7.01	4.63	3.9	0.623

Table I.2: Drought characteristics using a 90 percent fixed and variable threshold

		Mean duration [days]	Mean deficit $[\frac{m^3}{s}]$	No. of drought events
Beerze	Fixed	6.69	0.25	120
	Variable	8.59	0.86	255
Berkel	Fixed	4.91	1.07	176
	Variable	6.20	3.38	317
Bovenslinge	Fixed	6.22	0.22	110
	Variable	7.10	0.59	198
Dommel	Fixed	5.5	5.60	158
	Variable	6.41	7.96	270
Donge	Fixed	5.61	0.22	117
	Variable	6.39	0.60	208
Essche stroom	Fixed	6.27	1.27	114
	Variable	6.56	2.09	239
Geelebeek	Fixed	12.76	0.47	38
	Variable	9.40	1.08	123
Geleenbeek	Fixed	4.23	0.68	164
	Variable	5.16	1.51	470
Groenlosche Slinge	Fixed	6.25	0.61	84
	Variable	6.32	1.52	220
Geul	Fixed	4.96	0.96	179
	Variable	5.86	1.78	365
Hunze	Fixed	2.67	0.31	172
	Variable	3.49	0.53	360
Hupsel	Fixed	9.44	9.39×10^{-3}	80
	Variable	8.47	7.4×10^{-2}	229
Meuse	Fixed	3.24	17	256
	Variable	4.68	118.7	410
Nieuwe Leij	Fixed	8.35	0.30	94
	Variable	8.51	0.75	168
Oude IJssel	Fixed	6.62	3.53	107
	Variable	7.13	9.29	210
Regge	Fixed	3.68	2.47	179
	Variable	4.99	6.12	297
Reusel	Fixed	4.95	0.40	166
	Variable	5.94	0.91	313
Rhine	Fixed	14.68	2117	57
	Variable	13.56	2504	116
Roer	Fixed	5.63	7.41	164
	Variable	6.17	10.14	304
Schipbeek	Fixed	4.46	0.17	161
	Variable	6.60	1.09	321
Springendalsebeek	Fixed	4.60	2.4×10^{-2}	153
	Variable	4.96	2.6×10^{-2}	295
Tongelreep	Fixed	8.3	1.11	80
	Variable	6.15	0.60	215
Vecht	Fixed	7.13	7.55	68
	Variable	7.72	16.43	134